Contents

1. Failed Attempts S4

Scheme S1: Attempted synthesis of ruthenacarborane-(η^6-*p*-cymene)–NSAID conjugates from *nido*-carborate–NSAID conjugates. S4

Scheme S2: Attempted synthesis of ruthenacarborane alcohols S4

2. Cesium 1-(1'-Hydroxymethyl)-*nido*-carborane (**2a**): S5

Figure S1. ^{1}H NMR spectrum of **2a** in acetone-d_6. ..... S5

Figure S2. ^{11}B{^{1}H} NMR spectrum of **2a** in acetone-d_6 ..... S5

Figure S3. ^{13}C{^{1}H} NMR spectrum of **2a** in acetone-d_6 ..... S6

3. Cesium 1-(2'-Hydroxyethyl)-*nido*-carborane (**2b**) S7

Figure S4. ^{1}H NMR spectrum of **2b** in acetone-d_6. ..... S7

Figure S5. ^{11}B{^{1}H} NMR spectrum of **2b** in acetone-d_6. ..... S7

Figure S6. ^{13}C{^{1}H} NMR spectrum of **2b** in acetone-d_6. ..... S8

4. [Ru(η^6-*p*-cymene)-1-(1′-hydroxymethyl)-*closo*-$C_2B_9H_{10}$] (**3a**) S8

Figure S7. ^{1}H NMR spectrum of **3a** in $CDCl_3$. S9

Figure S8. ^{11}B{^{1}H} NMR spectrum of **3a** in $CDCl_3$. S9

Figure S9. ^{13}C{^{1}H} NMR spectrum of **3a** in $CDCl_3$. S10

5. [Ru(η^6-*p*-cymene){1-(2′-hydroxyethyl)-*closo*-$C_2B_9H_{10}$}] (**3b**) S10

Figure S10. ^{1}H NMR spectrum of **3b** in $CDCl_3$. S11

Figure S11. ^{11}B{^{1}H} NMR spectrum of **3b** in $CDCl_3$. S11

Figure S12. ^{13}C{^{1}H} NMR spectrum of **3b** in $CDCl_3$ S12

6. Ruthenacarborane-(*p*-cymene)–NSAID Conjugates S13

[Ru(η^6-*p*-cymene)-1-{methyl (*R/S*)-2-[4-(2-fluorobiphenyl-4-yl)propanoic acid ester]-*closo*-$C_2B_9H_{10}$}] (**4a**) S13

Figure S13. ^{1}H NMR spectrum of **4a** in $CDCl_3$. S13

Figure S14. $^{11}B\{^1H\}$ NMR spectrum of **4a** in $CDCl_3$. S13

Figure S15. $^{13}C\{^1H\}$ NMR spectrum of **4a** in $CDCl_3$ S14

[Ru(η^6-*p*-cymene)-2-{ethyl (*R/S*)-2-[4-(2-fluorobiphenyl-4-yl)propanoic acid ester]-*closo*-$C_2B_9H_{10}$}] (**4b**) S14

Figure S16. ^{1}H NMR spectrum of **4b** in $CDCl_3$. S14

Figure S17. $^{11}B\{^1H\}$ NMR spectrum of **4b** in $CDCl_3$. S15

Figure S18. $^{13}C\{^1H\}$ NMR spectrum of **4b** in $CDCl_3$. S15

[Ru(η^6-*p*-cymene)-2-[ethyl-2-(3-phenoxyphenyl)propanoic ester]-*closo*-$C_2B_9H_{10}$] (**5b**): S16

Figure S19. ^{1}H NMR spectrum of **5b** in $CDCl_3$. S16

Figure S20. $^{11}B\{^1H\}$ NMR spectrum of **5b** in $CDCl_3$. S16

Figure S21. $^{13}C\{^1H\}$ NMR spectrum of **5b** in $CDCl_3$. S17

[Ru(η^6-*p*-cymene)-2-{ethyl (*R/S*)-2-[4-(2-propylphenyl)propanoic acid ester]-*closo*-$C_2B_9H_{10}$}] (**6b**) S17

Figure S22. ^{1}H NMR spectrum of **6b** in $CDCl_3$. S17

Figure S23. $^{11}B\{^1H\}$ NMR spectrum of **6b** in $CDCl_3$. S18

Figure S24. $^{13}C\{^1H\}$ NMR spectrum of **6b** in $CDCl_3$. S18

7. Comparison between ruthenacarborane (**3a**) and ruthenacarborane-(η^6-*p*-cymene)−NSAID conjugates with flurbiprofen (**4a**) S19

Figure S25. Comparison between ruthenium complexes **3a** and **4a**. S19

8. Stability Test S20

Figure S26. Stability of compound **4a** over 72 h in DMSO (^{1}H NMR spectroscopy). S20

9. UV-VIS Spectroscopy S20

Figure S27. UV/Vis spectra of **4a**, **5b** and **6b** at pH 4 and 7 at 0, 24 and 48 h. S20

10. Analysis of Purity by High-Performance Liquid Chromatography (HPLC) S21

Table S1. Results of HPLC analyses of ibuprofen, fenoprofen, flurbiprofen, **2a**, **2b**, **3a**, **3b**, **4a**, **4b**, **5b** and **6b** at 220 and 254 nm. S21

11. Evaluation for COX Inhibition S23

Figure S28. COX-2 inhibition data of **2b**. S23

12. Dynamic Light Scattering (DLS) Measurements S23

Figure S29: Count of particles of compound **4a**, **4b**, **5b** and **6b** STD (200 nm) and solvent (DMSO + PBS). S23

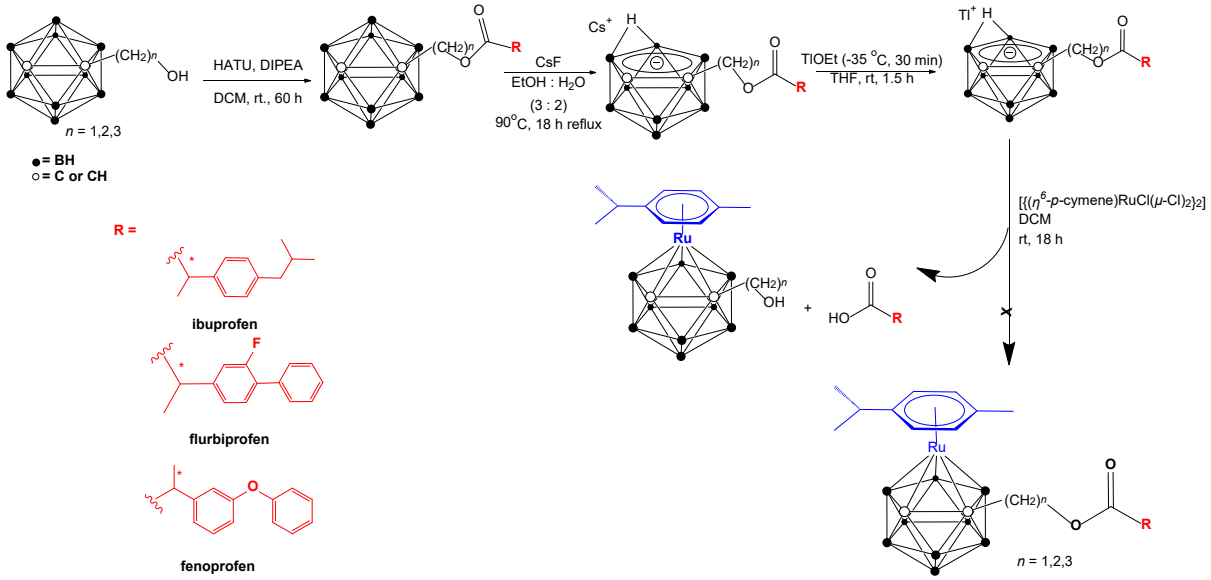
Table S2. Total number concentration and particles concentration peak of compound **4a**, **4b**, **5b** and **6b** particles (200 nm) and solvent (DMSO + PBS). S24

13. Cyclic Voltammetry (CV) S24

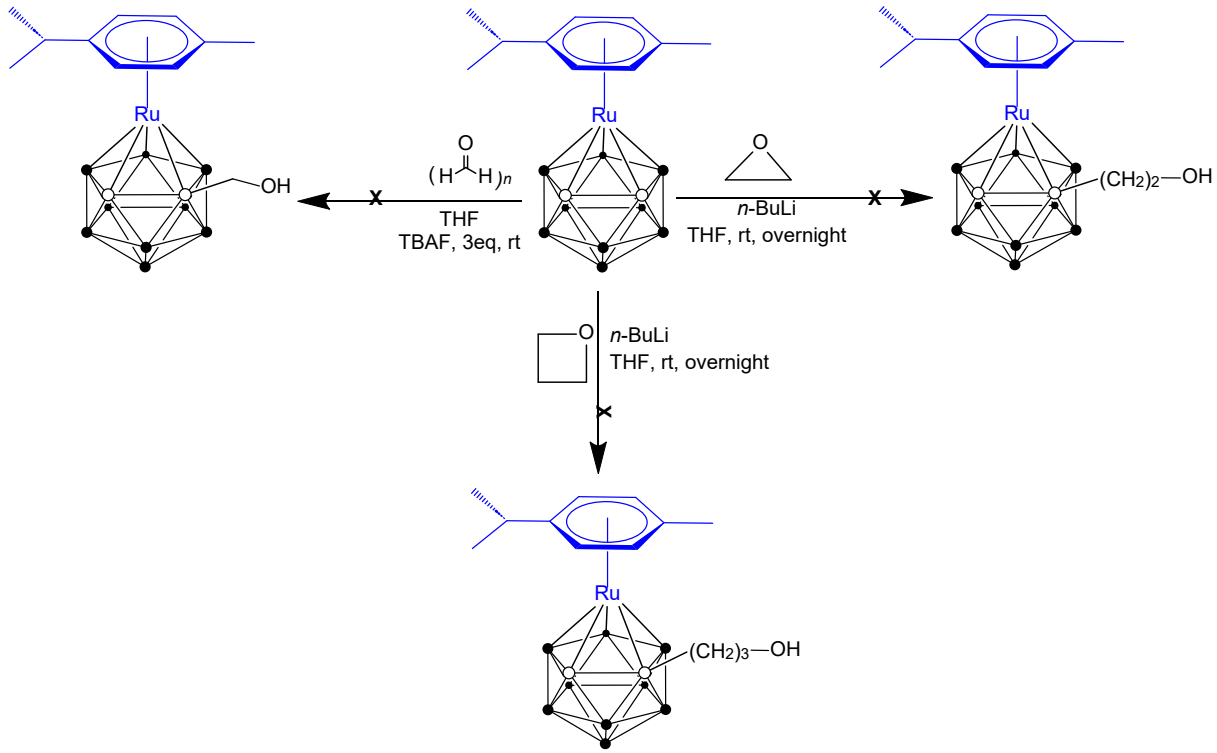
Figure S30. Comparison of CVs obtained for **4a**, **5b**, and **6b**. S24

Figure S31. Cyclic voltammograms at different current of **4a**, **5b**, and **6b**. S25
14. Cell Viability S26
Figure S32. The effect of **2a** and **2b** on the viability of human cancer cell lines and primary transformed lung embryonal fibroblasts..... S26
Figure S33. The effect of **3a** and **3b** on the viability of human cancer cell lines and primary transformed lung embryonal fibroblasts. S27
Figure S34. The effect of **4a**, **4b**, **5b**, and **6b** on the viability of human cancer cell lines and primary transformed lung embryonal fibroblasts S28
15. Stability Test by UPLC-MS S29
Table S3: Stability test by UPLC-MS. Compounds, retention times and m/z. S29
Figure S35: Stability studies of compound **4a** in various media over 48 h. S30
Figure S36: Stability studies of compound **5b** in various media over 48 h. S31
Figure S37: Stability studies of compound **6b** in various media over 48 h. S32

1. Failed Attempts



Scheme S1: Attempted synthesis of ruthenacarborane-(η^6-*p*-cymene)–NSAID conjugates from *nido*-carborate–NSAID conjugates.



Scheme S2: Attempted synthesis of ruthenacarborane alcohols.

2. Cesium 1-(1'-Hydroxymethyl)-*nido*-carborane (**2a**)

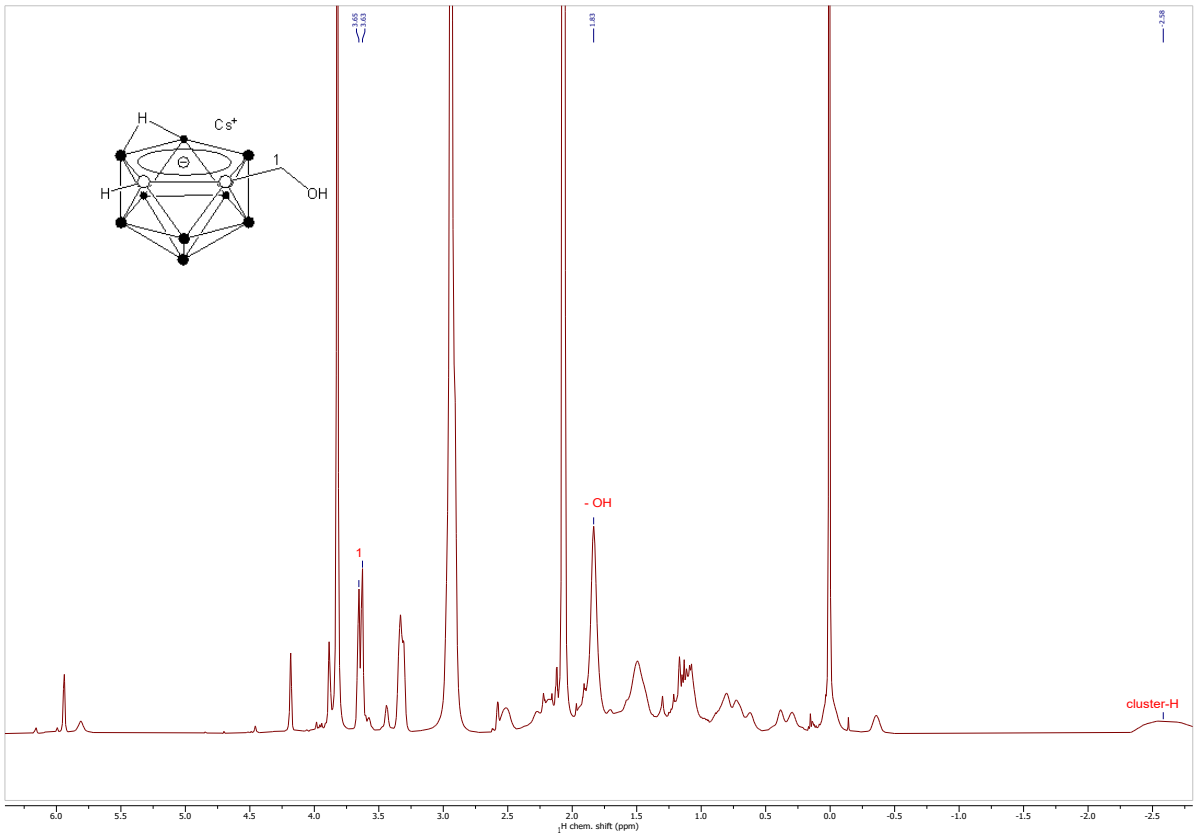


Figure S1. ^{1}H NMR spectrum of **2a** in acetone-d_6.

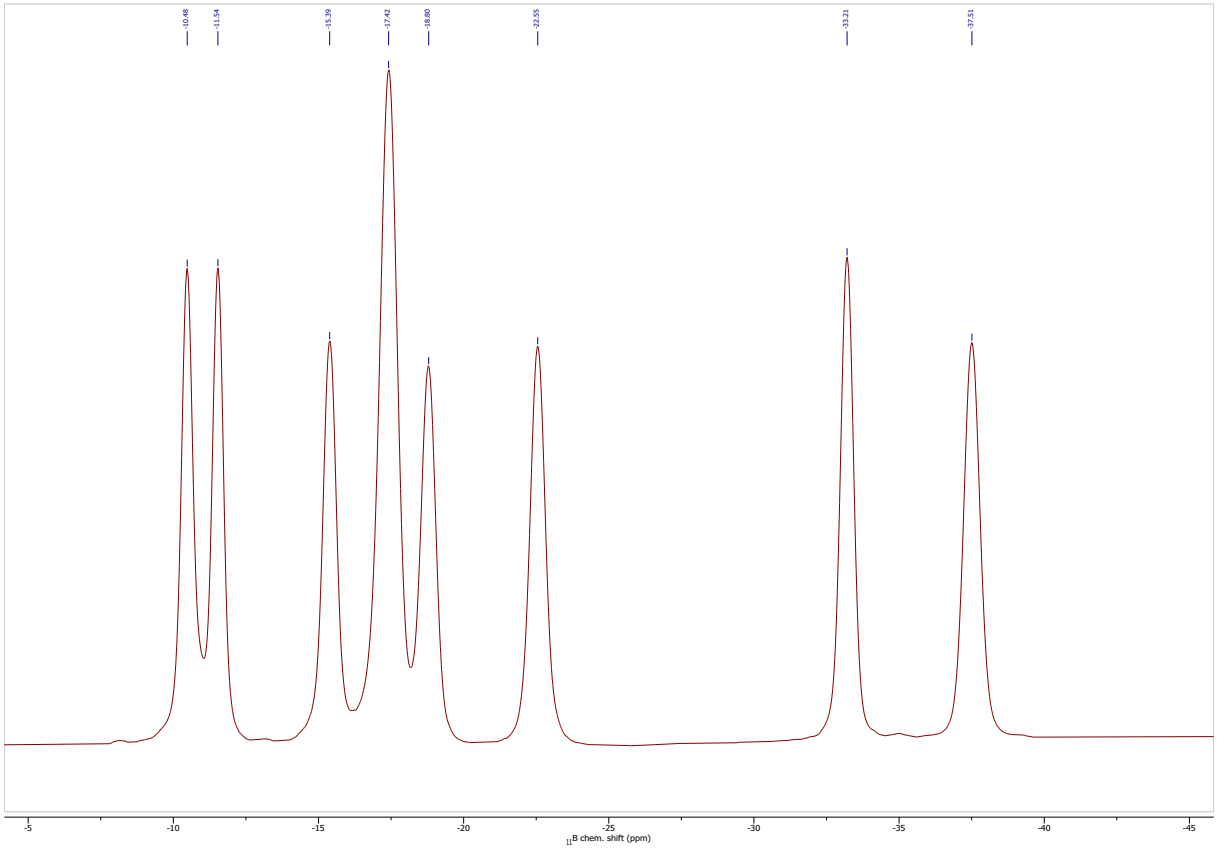


Figure S2. ^{11}B{^{1}H} NMR spectrum of **2a** in acetone-d_6.

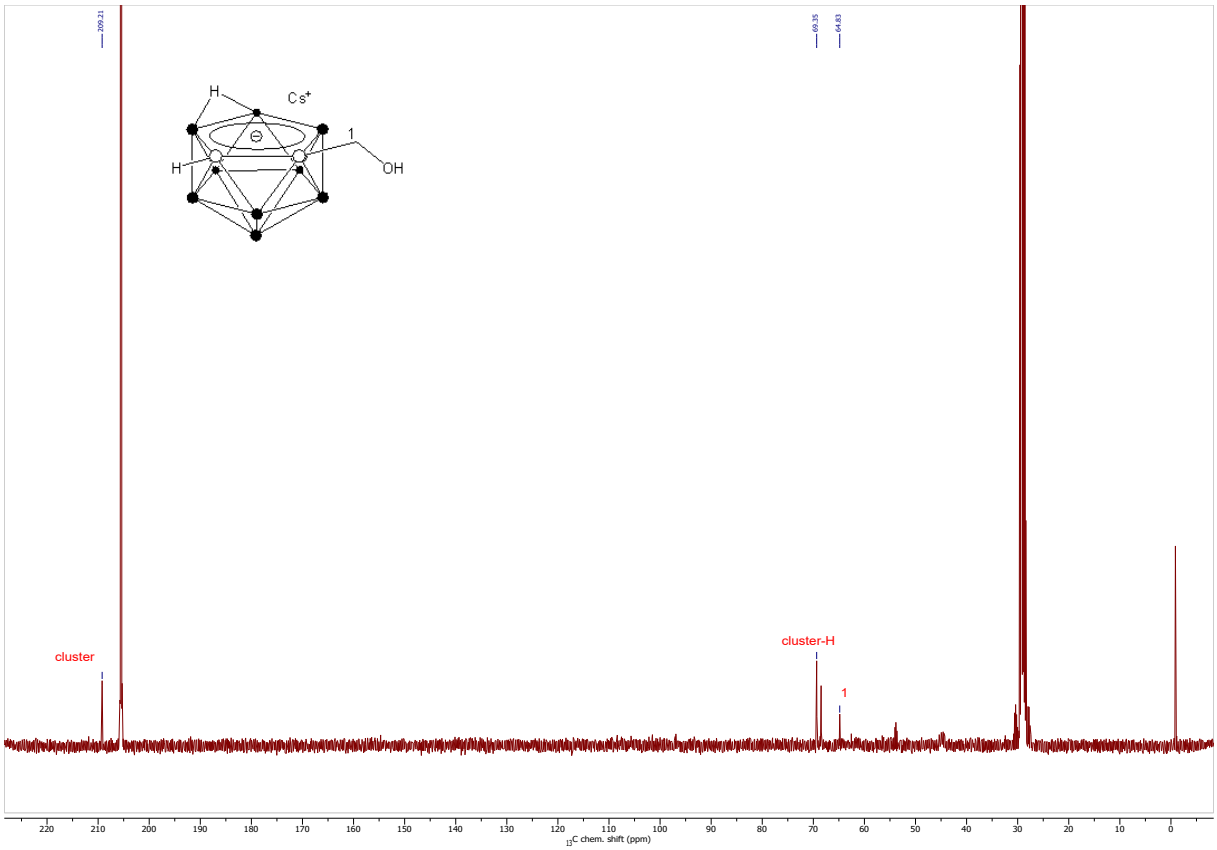


Figure S3. $^{13}C\{^{1}H\}$ NMR spectrum of **2a** in acetone-d_6.

3. Cesium 1-(2'-Hydroxyethyl)-*nido*-carborane (**2b**)

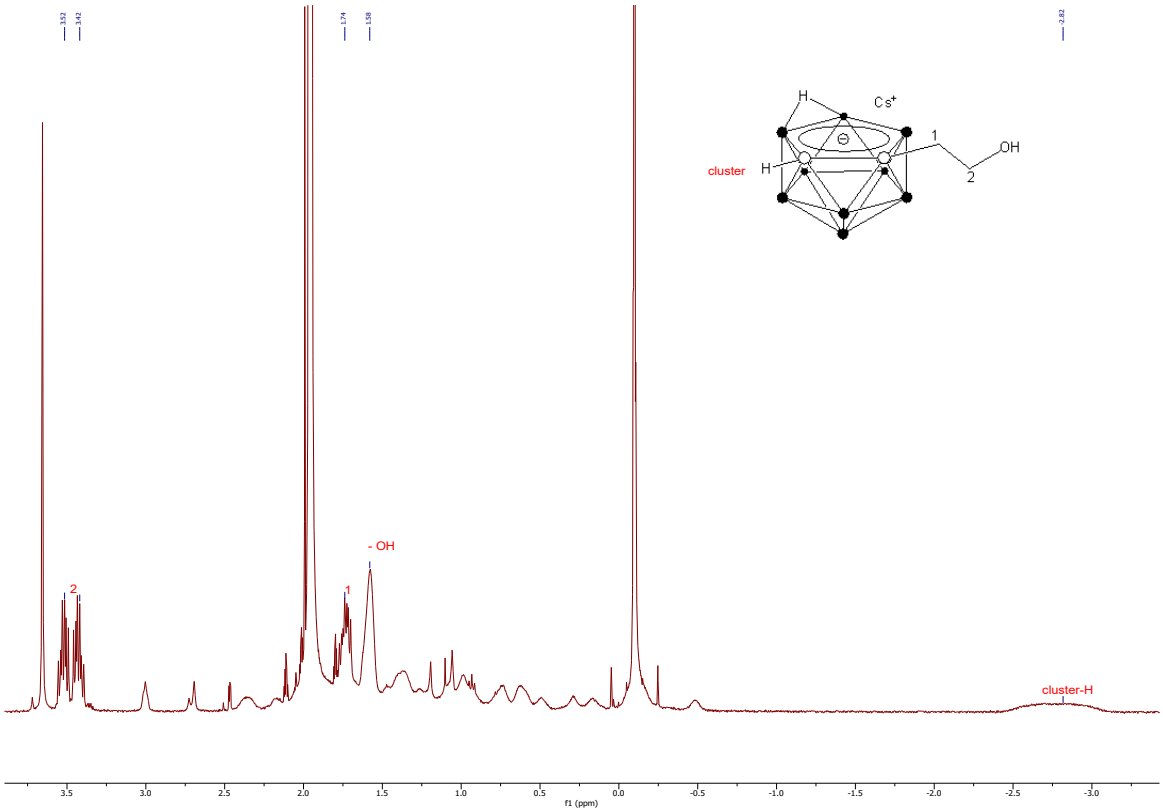


Figure S4. ^{1}H NMR spectrum of **2b** in acetone-d_6.

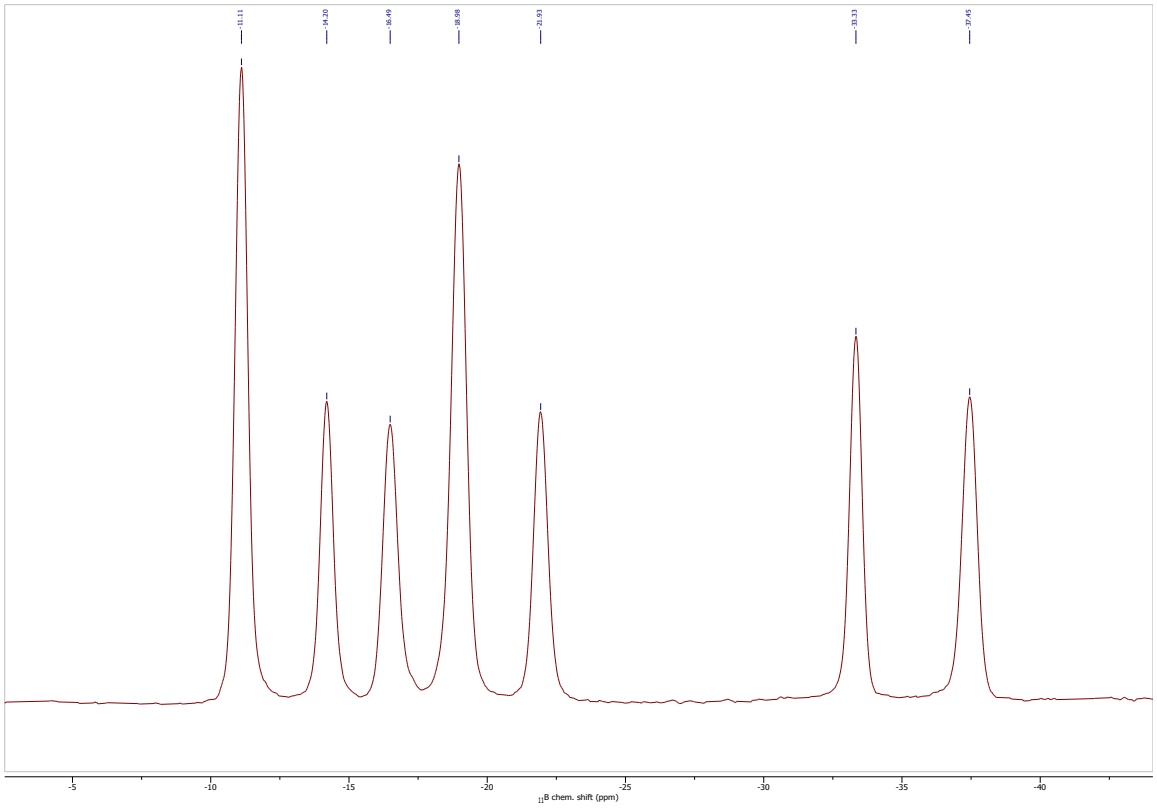


Figure S5. ^{11}B{^{1}H} NMR spectrum of **2b** in acetone-d_6.

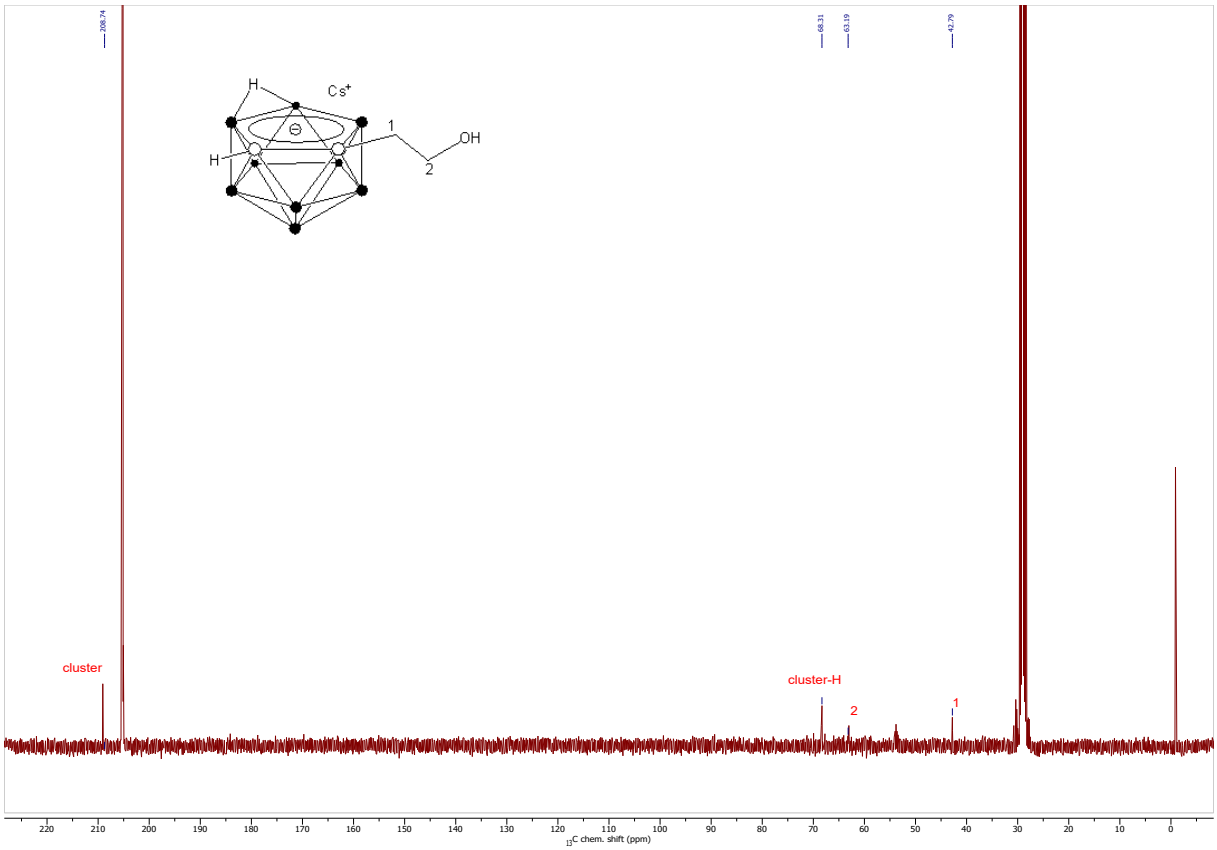


Figure S6. $^{13}C\{^{1}H\}$ NMR spectrum of **2b** in acetone-d_6.

4. [Ru(η^6-*p*-cymene){1-(1′-hydroxymethyl)-*closo*-$C_2B_9H_{10}$}] (**3a**):

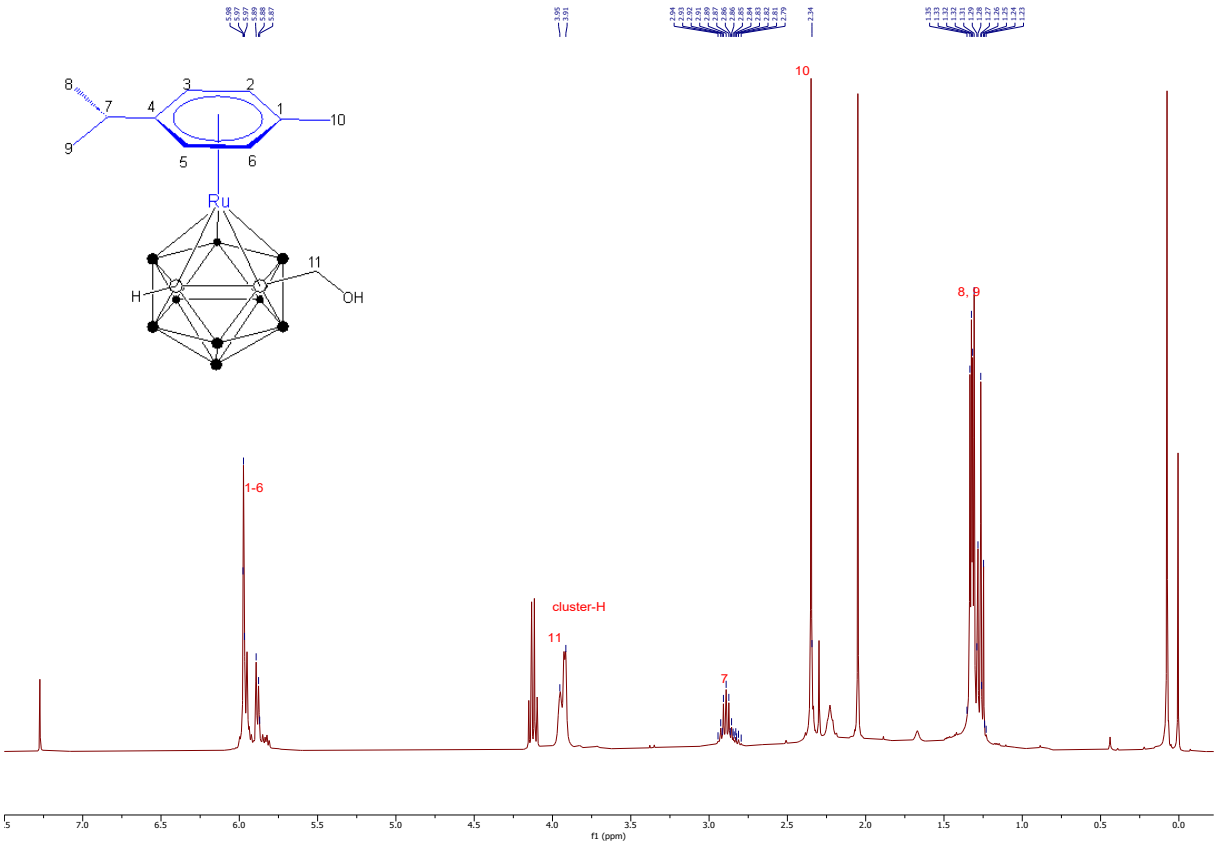


Figure S7. ^{1}H NMR spectrum of **3a** in $CDCl_3$.

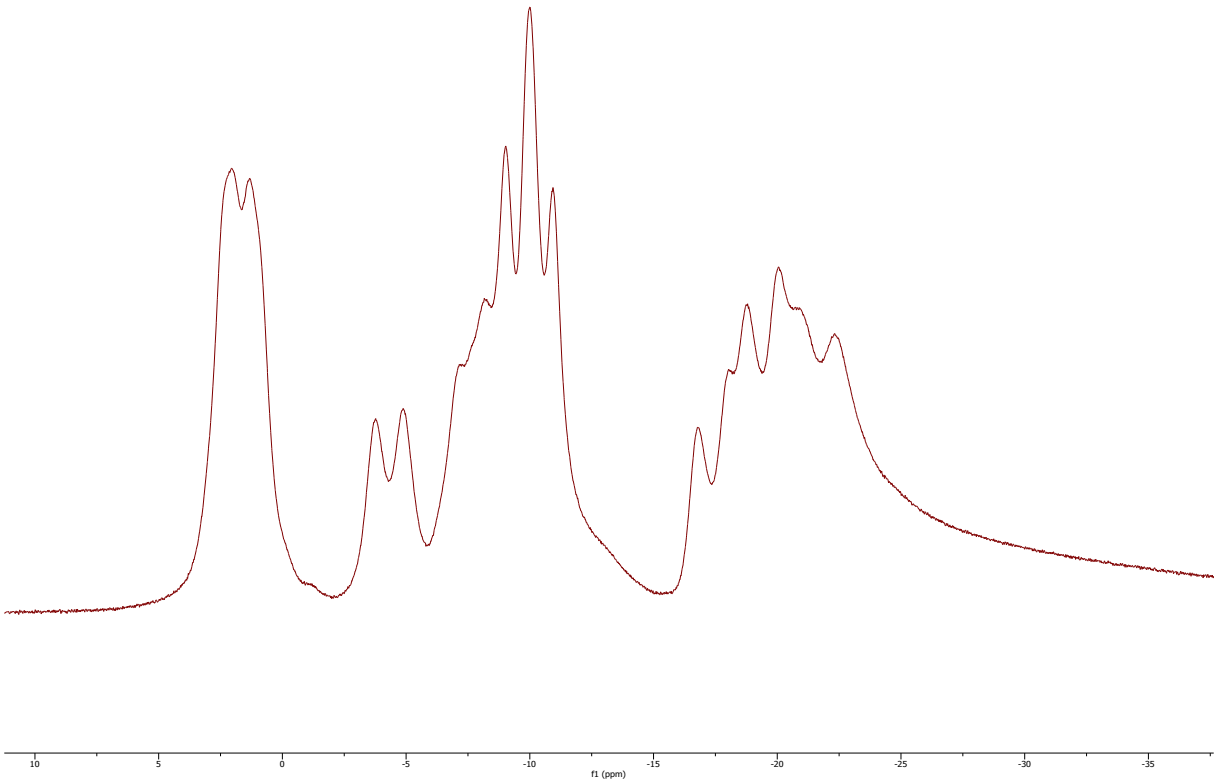


Figure S8. $^{11}B\{^{1}H\}$ NMR spectrum of **3a** in $CDCl_3$.

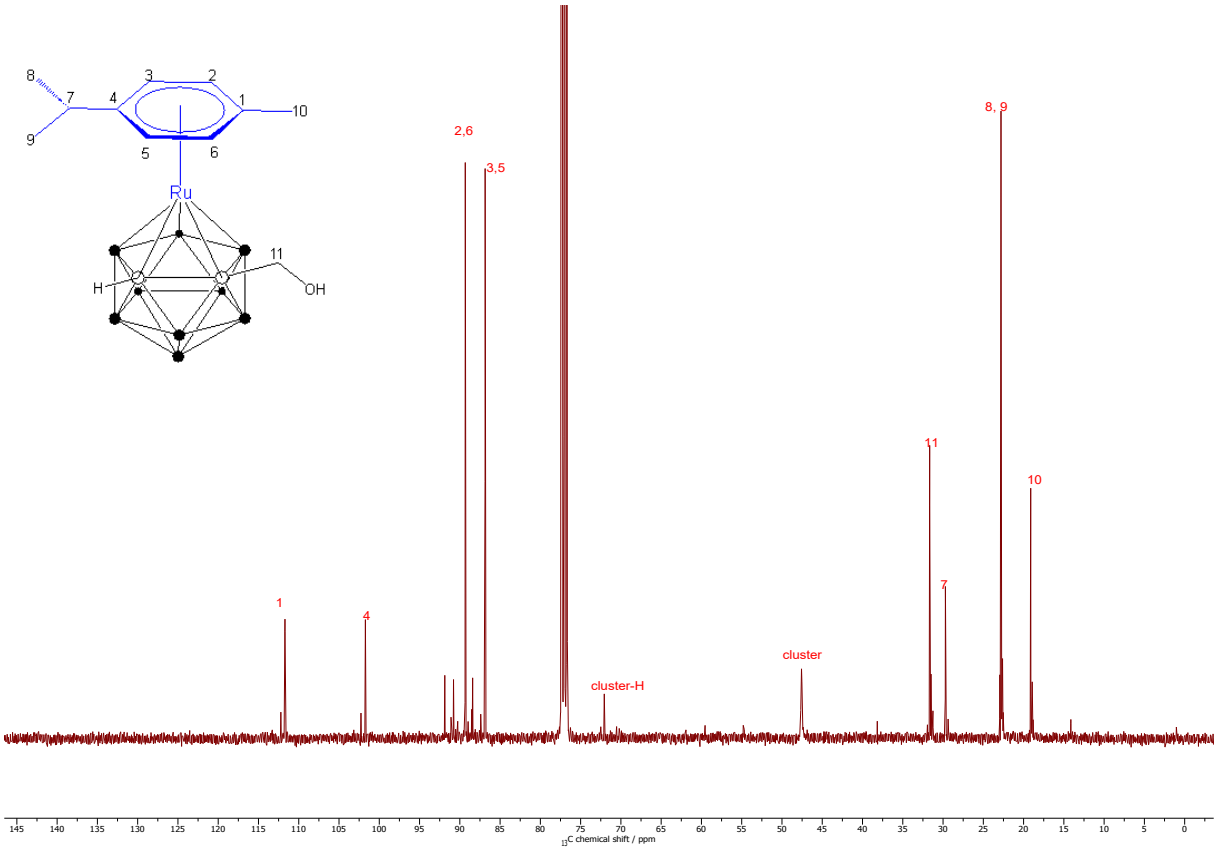


Figure S9. $^{13}C\{^{1}H\}$ NMR spectrum of **3a** in $CDCl_3$.

5. [Ru(η^6-*p*-cymene){1-(2′-hydroxyethyl)-*closo*-$C_2B_9H_{10}$}] (**3b**)

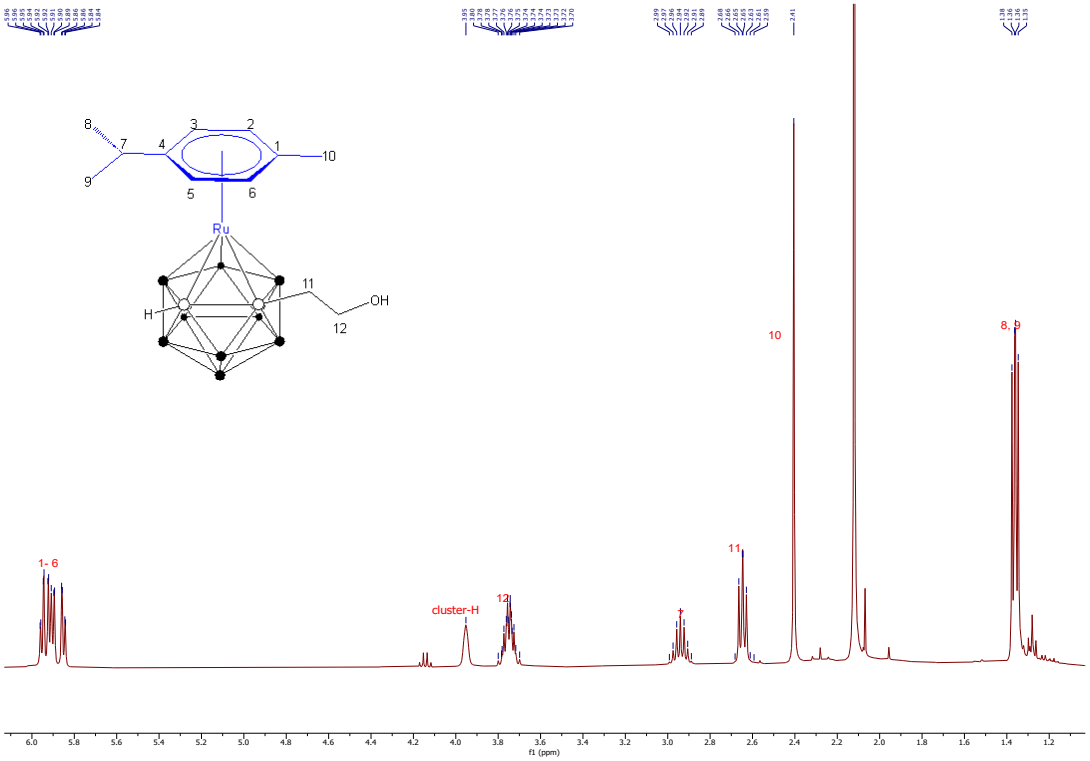


Figure S10. ^{1}H NMR spectrum of **3b** in $CDCl_3$.

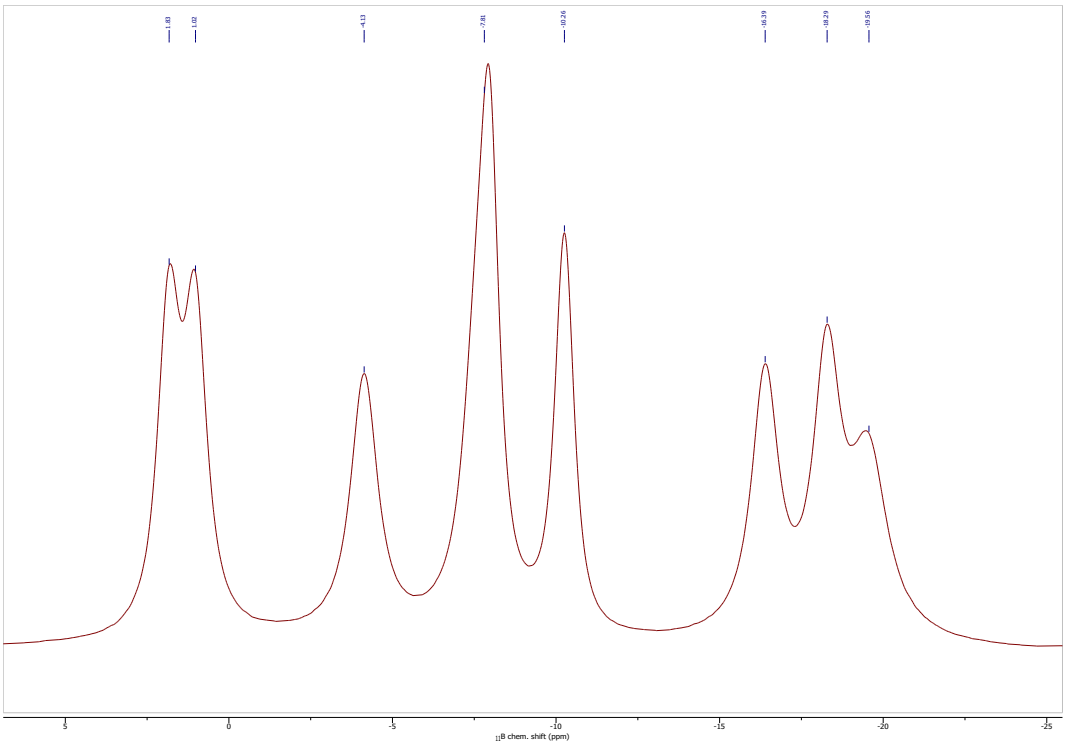
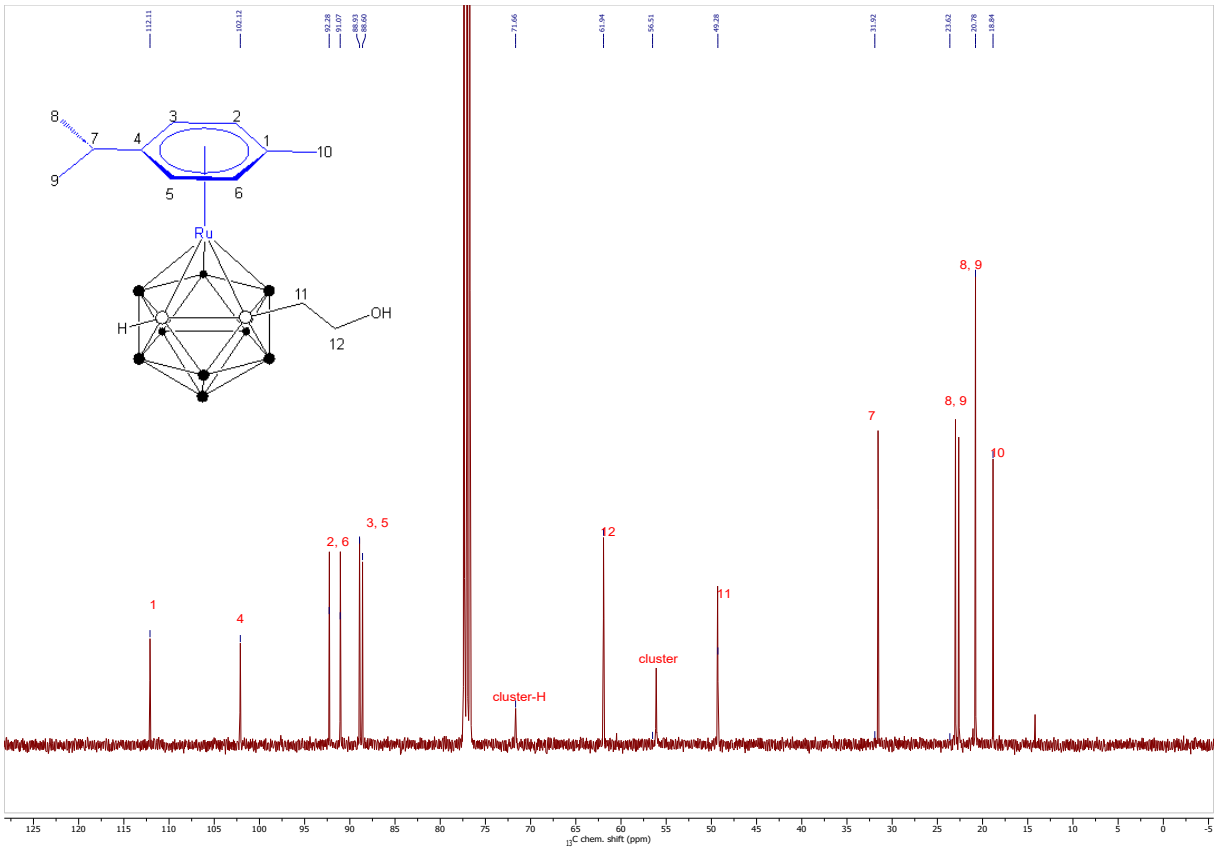


Figure S11. $^{11}B\{^{1}H\}$ NMR spectrum of **3b** in $CDCl_3$.



S

Figure S12. $^{13}C\{^{1}H\}$ NMR spectrum of **3b** in $CDCl_3$

6. Ruthenacarborane-(*p*-cymene)–NSAID Conjugates

[Ru(η^6-*p*-cymene){1-methyl (*R/S*)-2-[4-(2-fluorobiphenyl-4-yl)propanoic acid ester]-*closo*-$C_2B_9H_{10}$}] (**4a**):

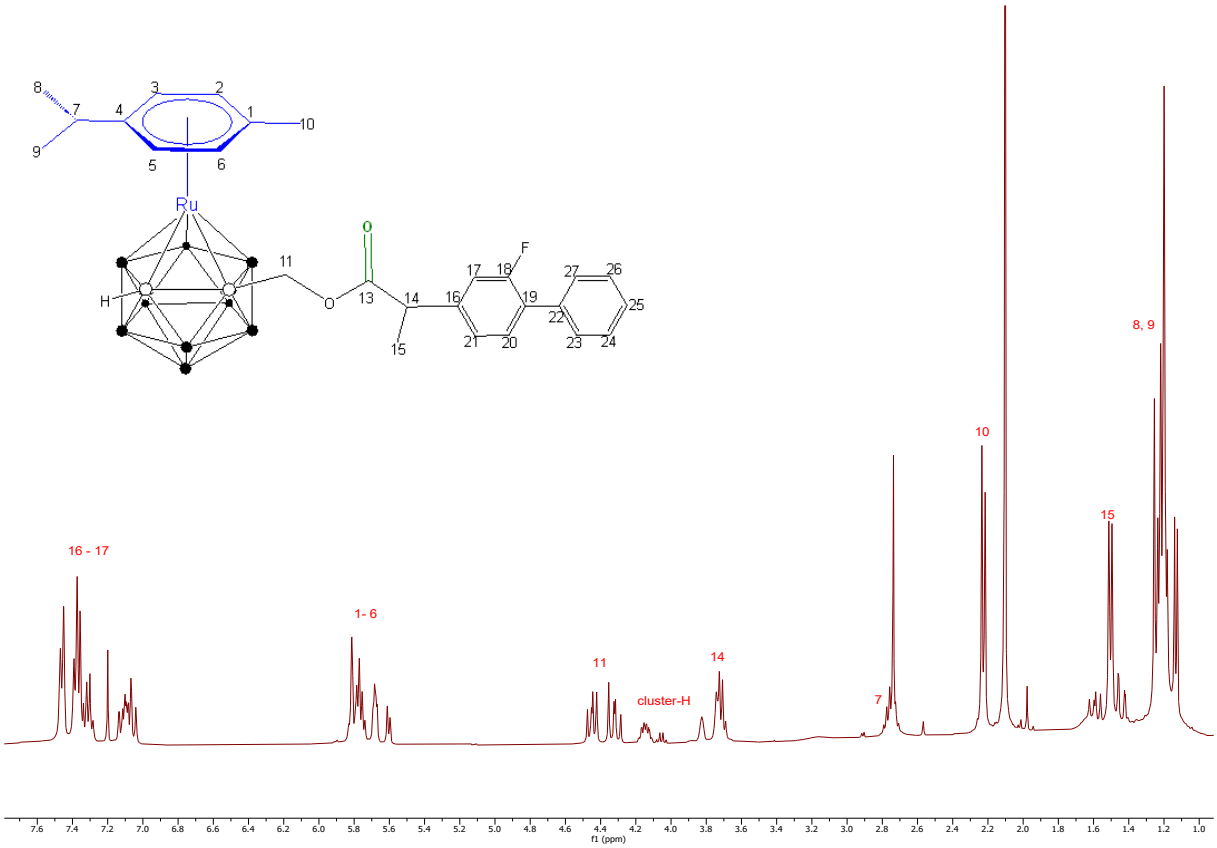


Figure S13. ^{1}H NMR spectrum of **4a** in $CDCl_3$..

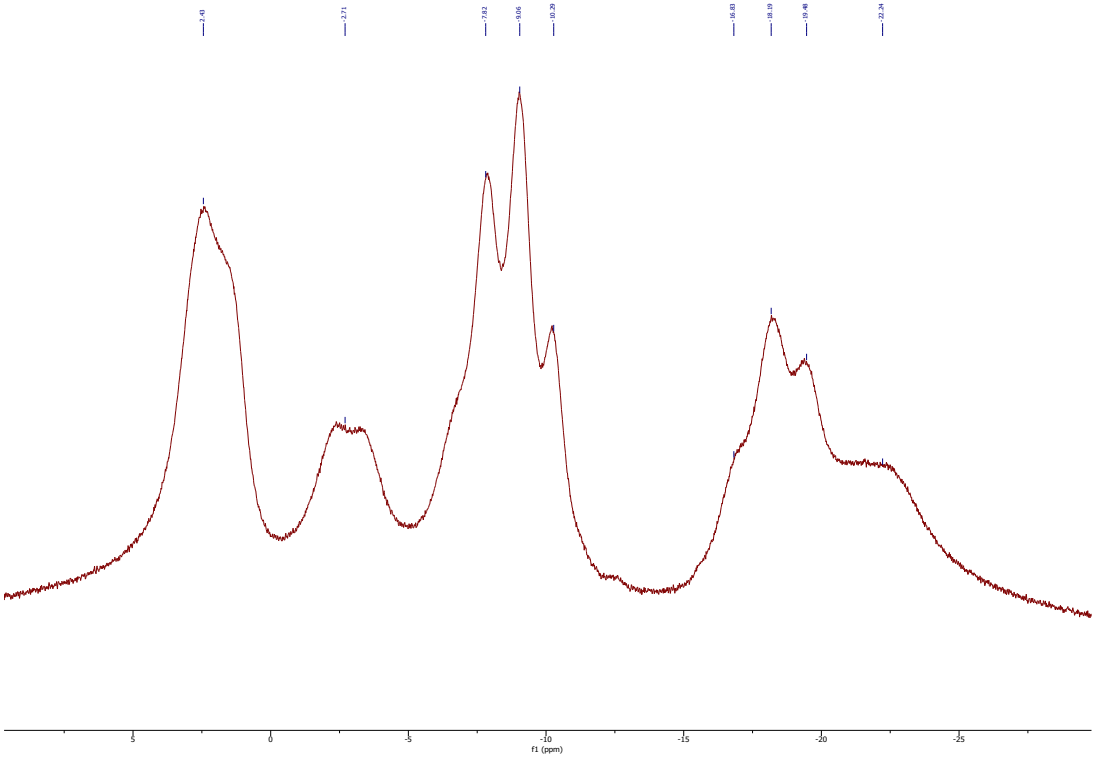


Figure S14. $^{11}B\{^{1}H\}$ NMR spectrum of **4a** in $CDCl_3$.

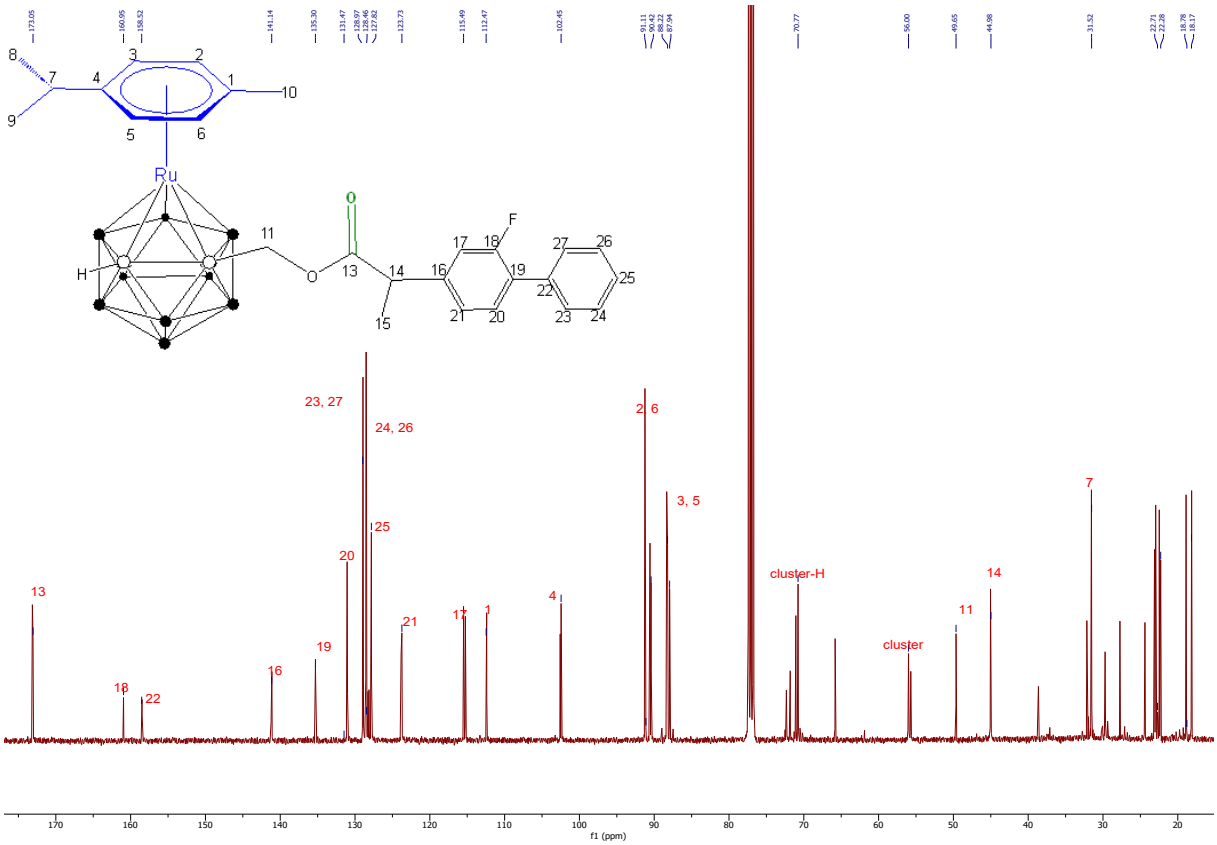


Figure S15. $^{13}C\{^{1}H\}$ NMR spectrum of **4a** in $CDCl_3$.

[Ru(η^6-*p*-cymene){2-ethyl (*R/S*)-2-[4-(2-fluorobiphenyl-4-yl)propanoic acid ester]-*closo*-$C_2B_9H_{10}$}] (**4b**):

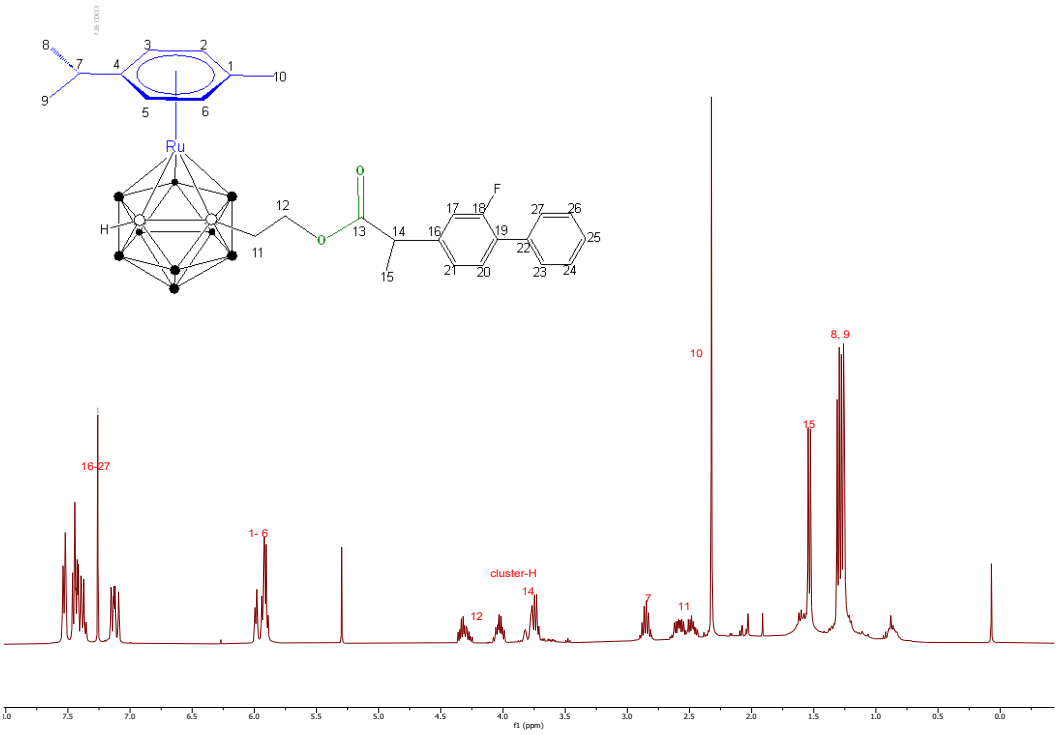


Figure S16. ^{1}H NMR spectrum of **4b** in $CDCl_3$.

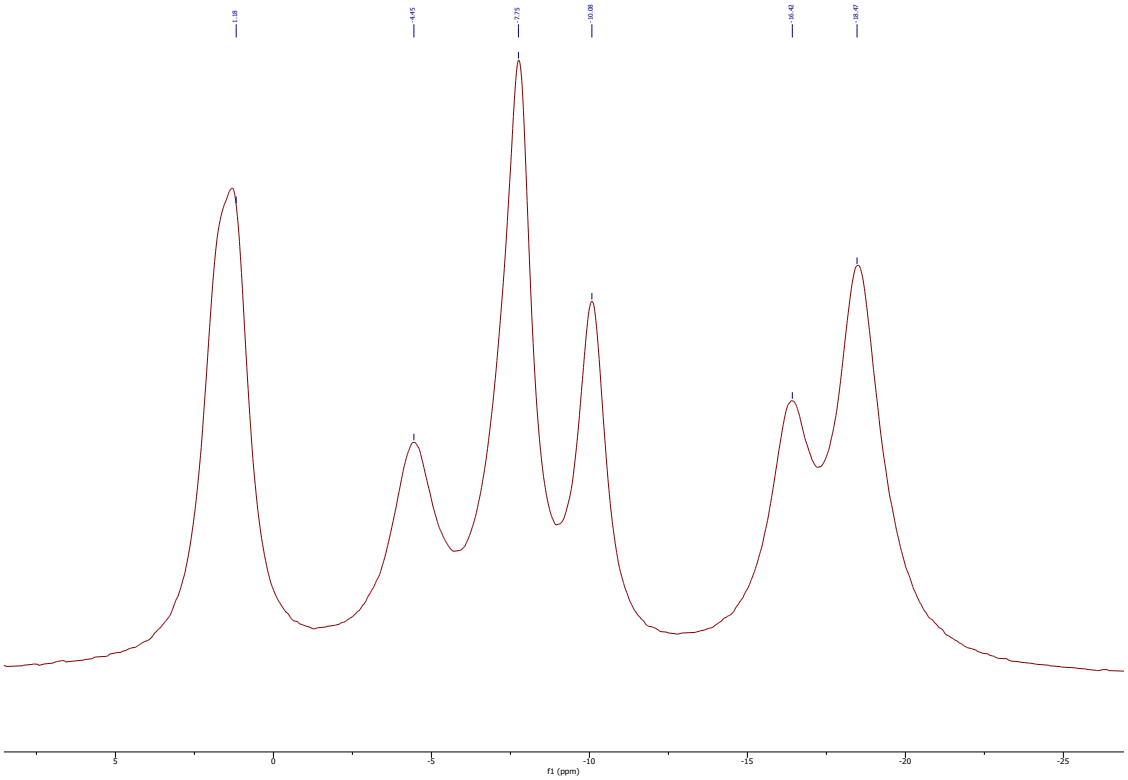


Figure S17. $^{11}B\{^1H\}$ NMR spectrum of **4b** in $CDCl_3$.

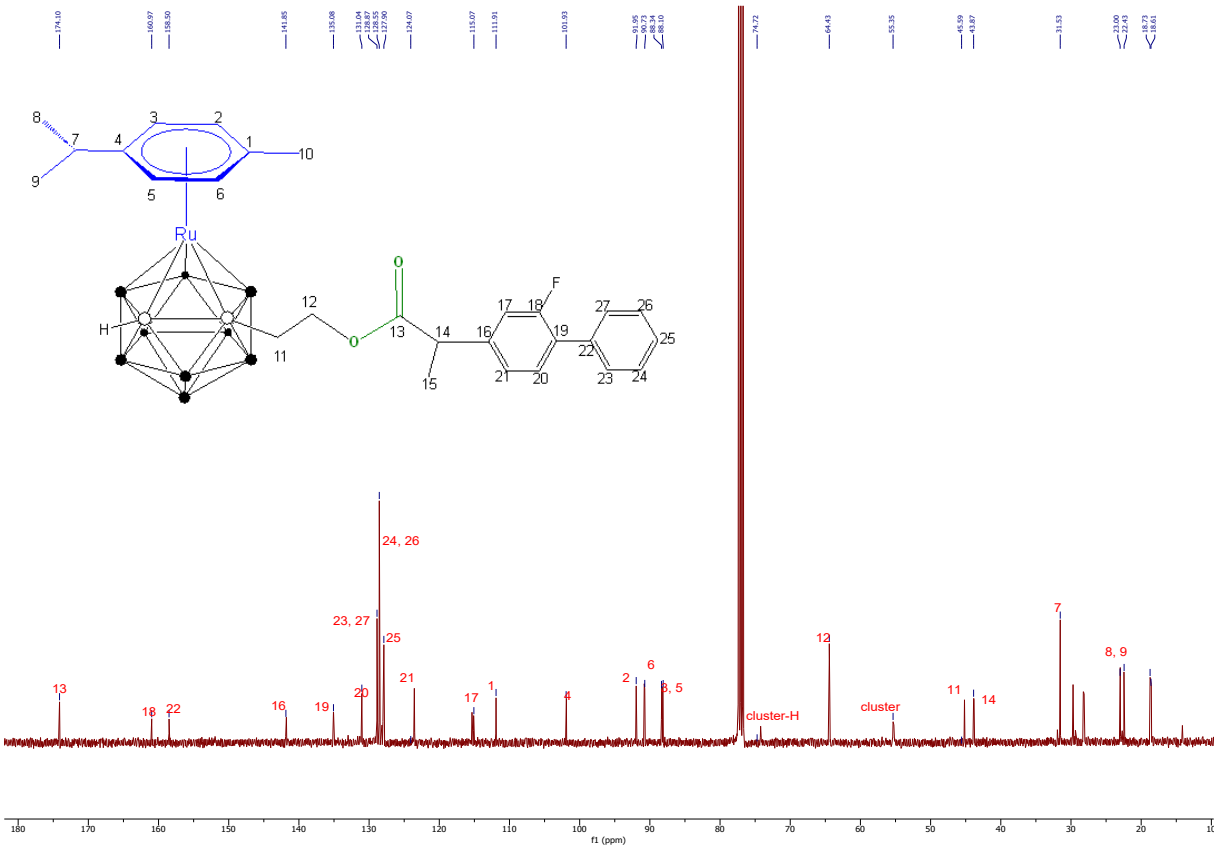


Figure S18. $^{13}C\{^1H\}$ NMR spectrum of **4b** in $CDCl_3$.

[Ru(η^6-*p*-cymene){2-ethyl [2-(3-phenoxyphenyl)propanoic acid ester]-*closo*-$C_2B_9H_{10}$}] (**5b**):

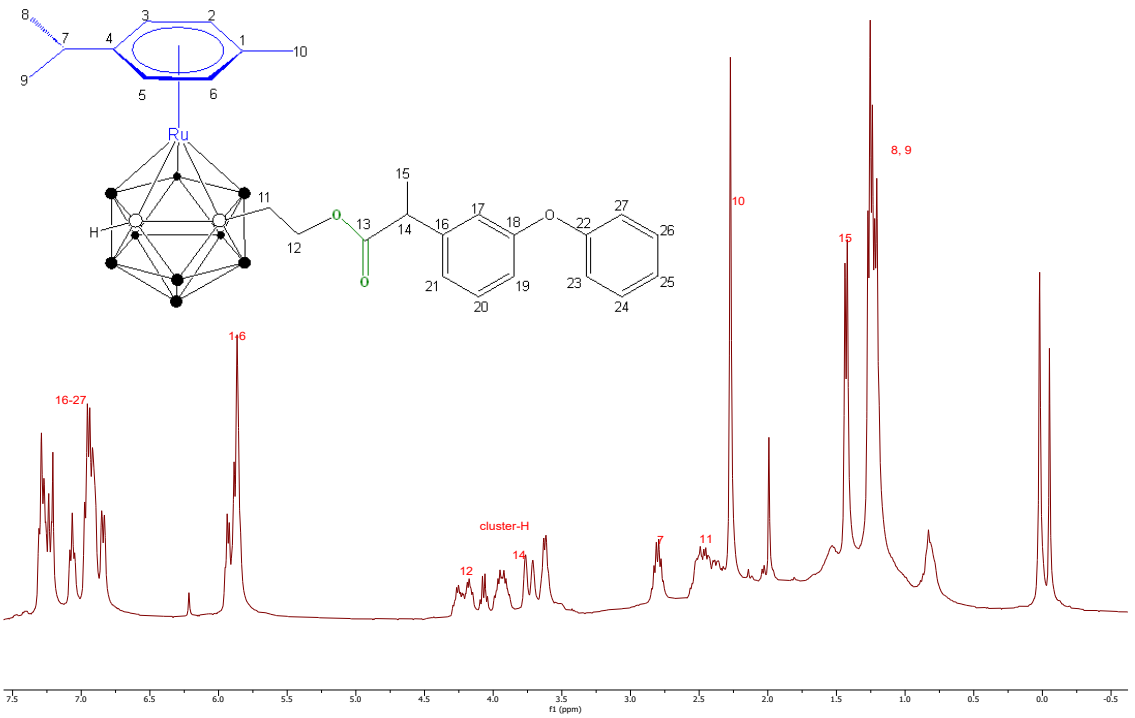


Figure S19. ^{1}H NMR spectrum of **5b** in $CDCl_3$.

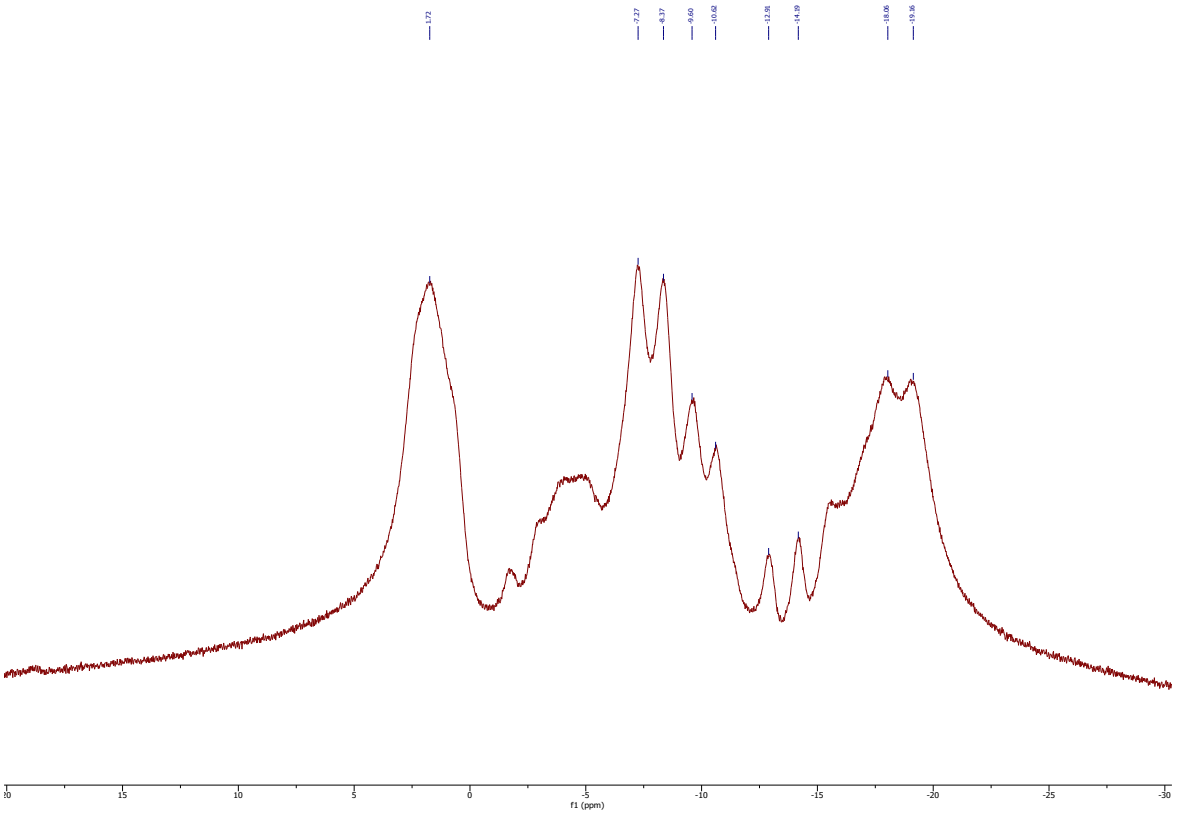


Figure S20. $^{11}B\{^{1}H\}$ NMR spectrum of **5b** in $CDCl_3$.

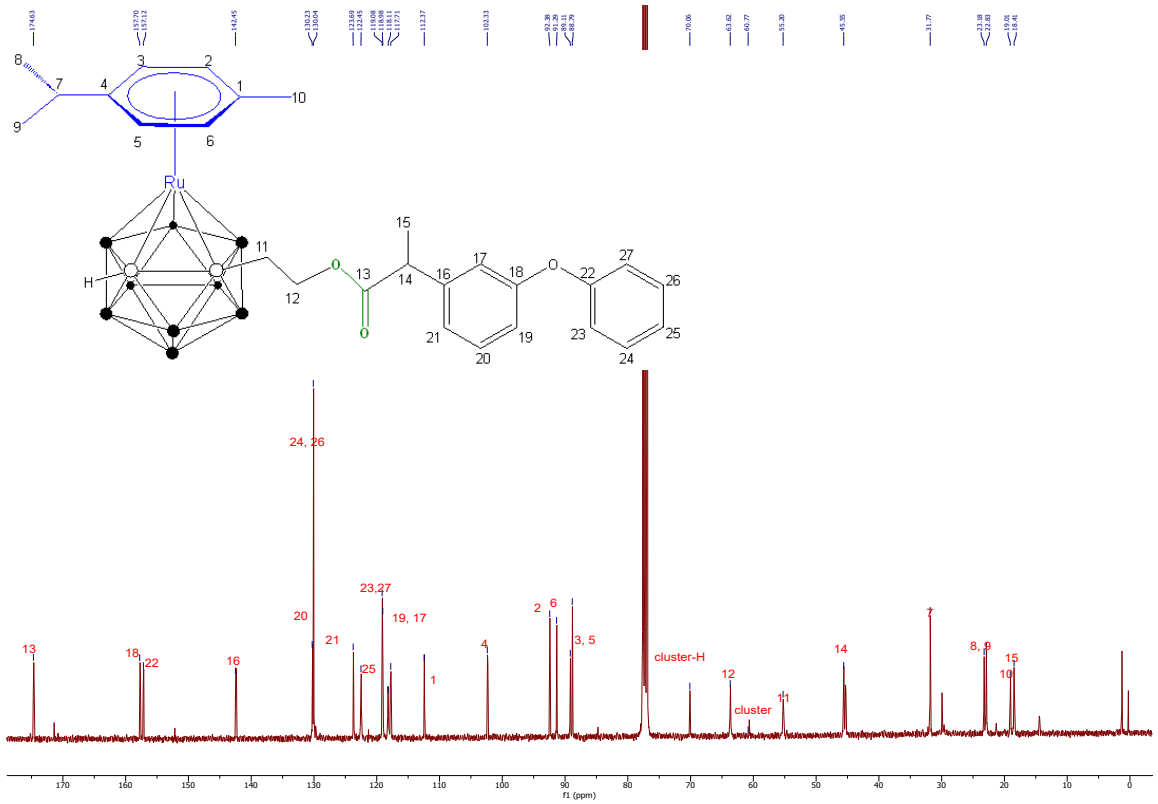


Figure S21. $^{13}C\{^{1}H\}$ NMR spectrum of **5b** in $CDCl_3$.

[Ru(η^6-*p*-cymene){2-ethyl (*R/S*)-2-[4-(2-propylphenyl)propanoic acid ester]-*closo*-$C_2B_9H_{10}$}] (**6b**):

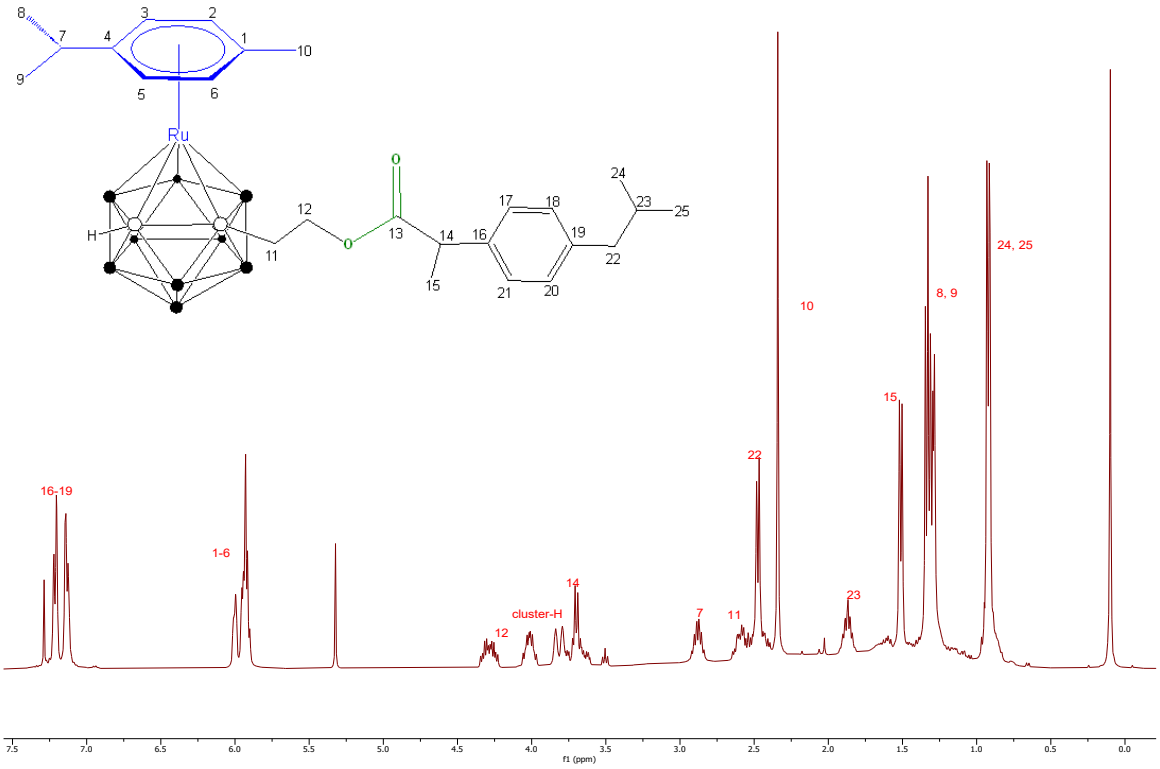


Figure S22. ^{1}H NMR spectrum of **6b** in $CDCl_3$.

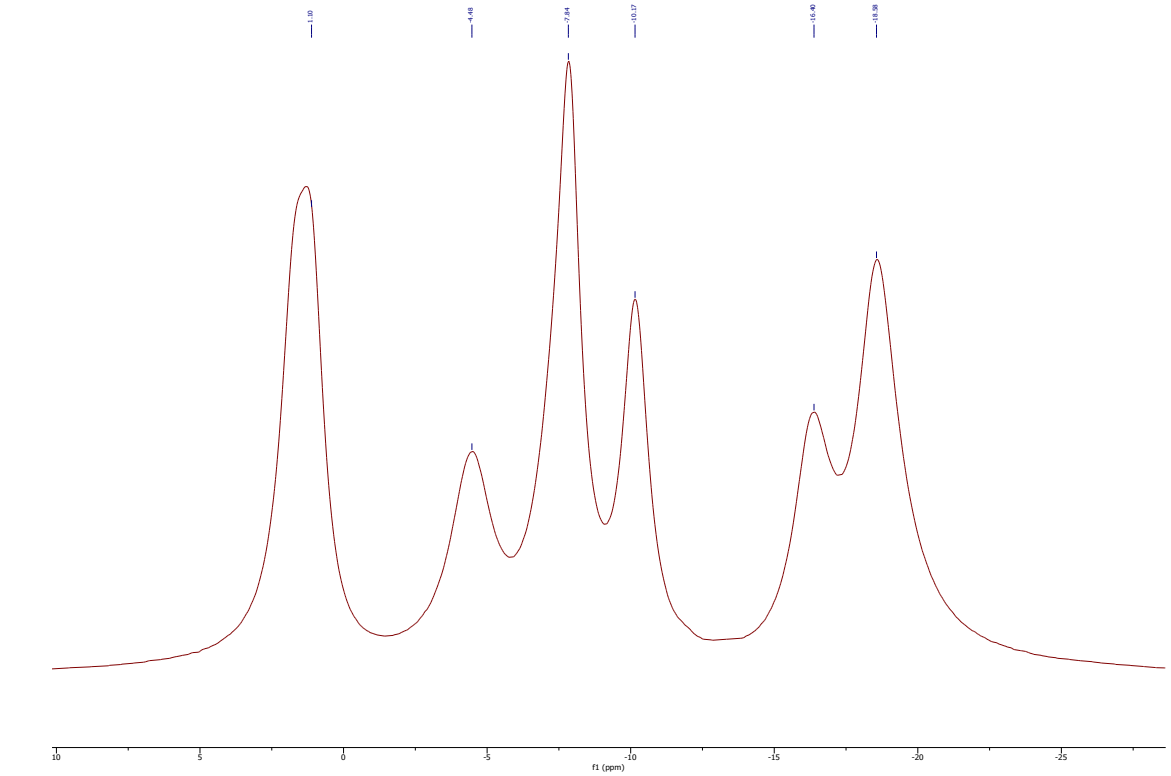


Figure S23. $^{11}B\{^{1}H\}$ NMR spectrum of **6b** in $CDCl_3$.

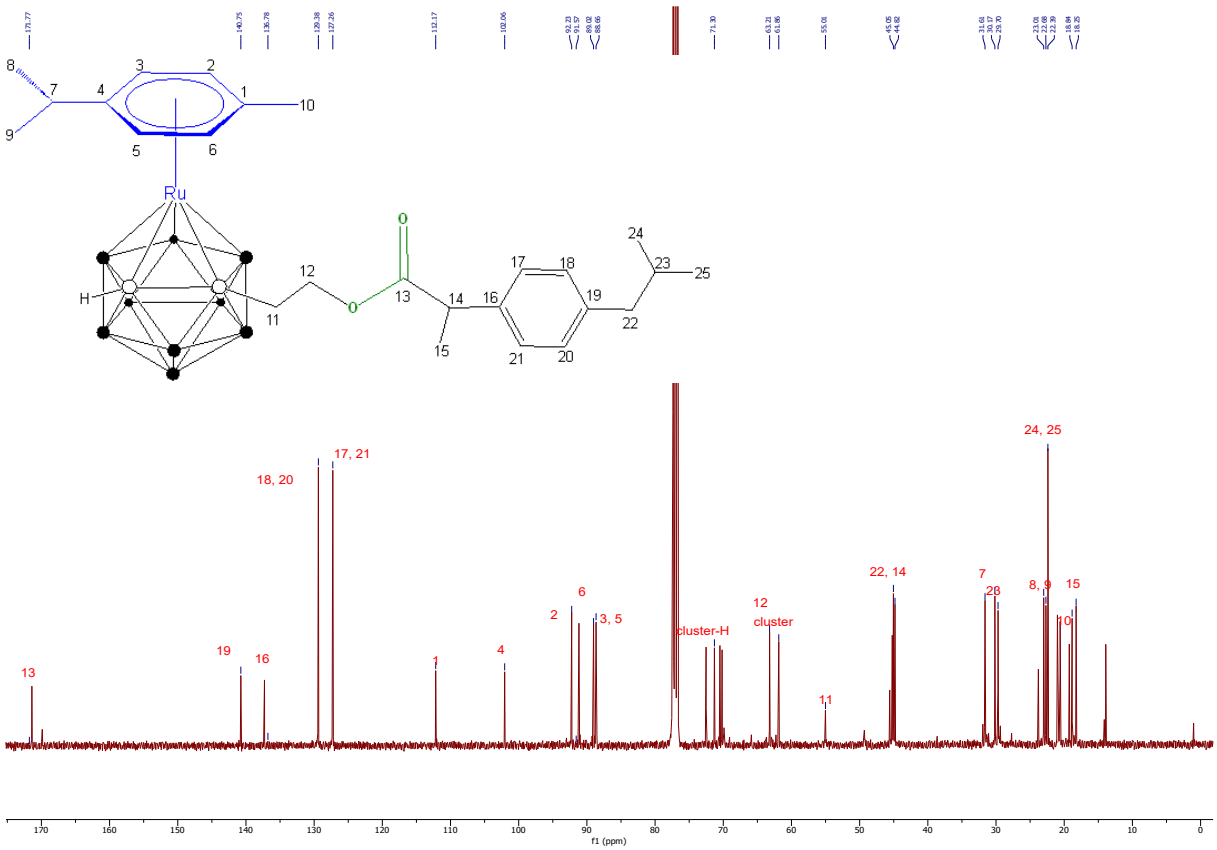


Figure S24. $^{13}C\{^{1}H\}$ NMR spectrum of **6b** in $CDCl_3$.

7. Comparison between ruthenacarborane (**3a**) and ruthenacarborane-(η^6-*p*-cymene)–NSAID conjugates with flurbiprofen (**4a**)

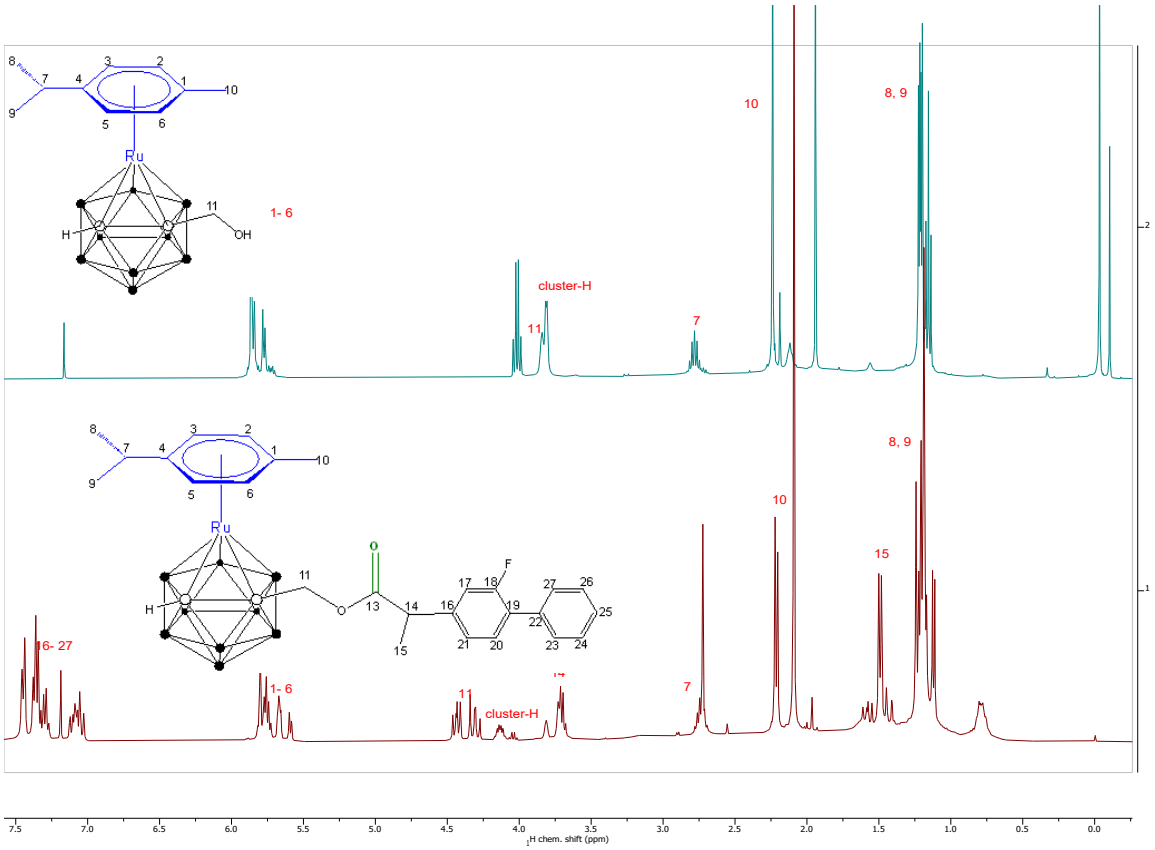


Figure S25. Comparison between ruthenium complexes **3a** (top) and **4a** (bottom).

8. Stability Test

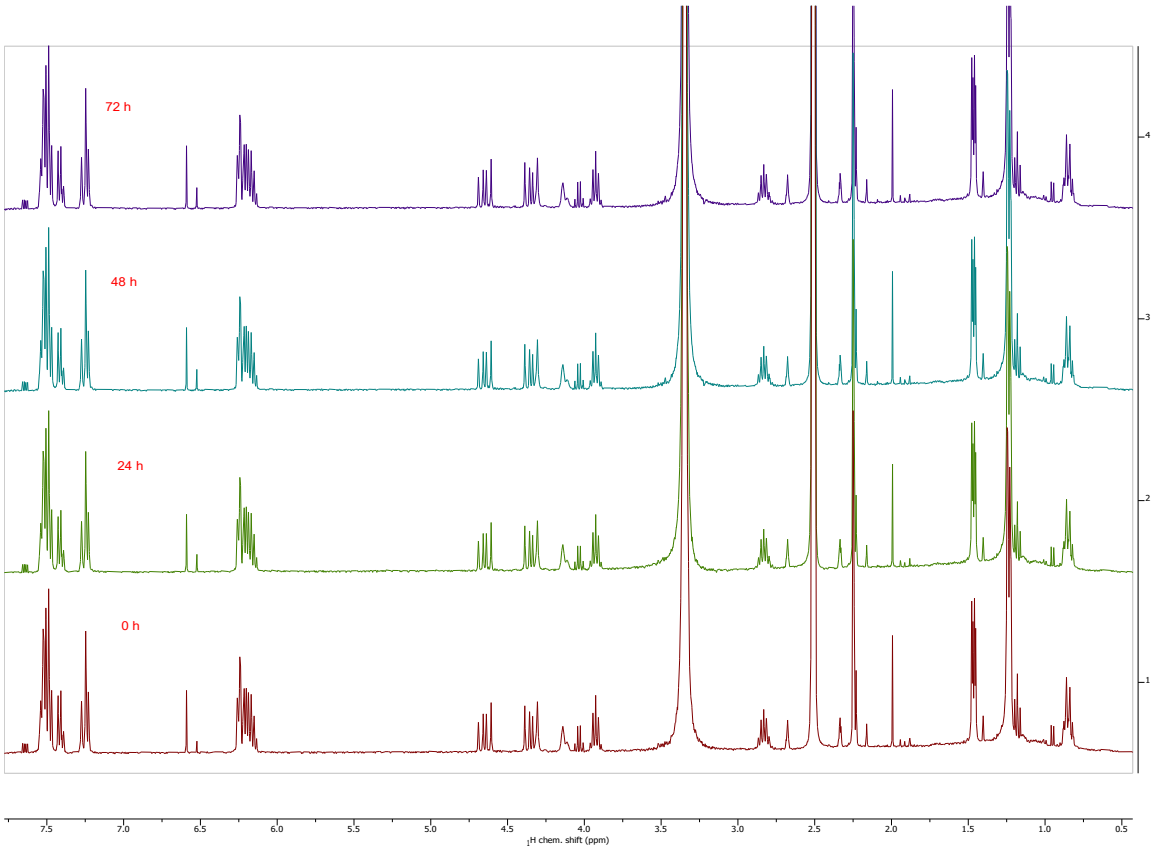


Figure S26. Stability of compound **4a** over 72 h in DMSO-d_6 (^{1}H NMR spectroscopy). Compound **4a** was dissolved in deuterated DMSO and stored at room temperature. ^{1}H NMR spectroscopy was performed at selected time intervals (0, 24, 48 and 72 h).

9. UV-VIS Spectroscopy

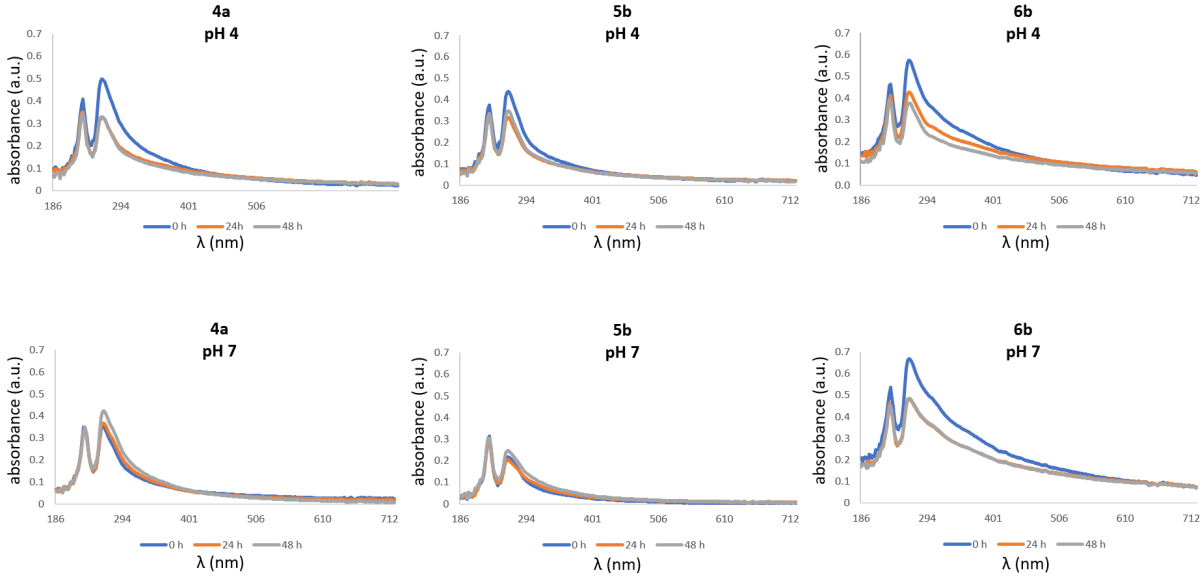
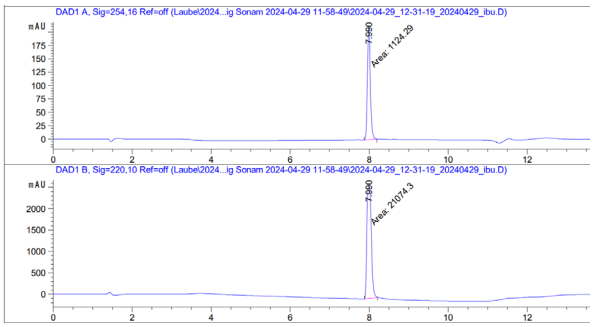


Figure S27. UV/Vis spectra of **4a**, **5b** and **6b** at pH 4 and 7 at 0, 24 and 48 h.

10. Analysis of Purity by High-Performance Liquid Chromatography (HPLC)

Table S1. Results of HPLC analyses of ibuprofen, fenoprofen, flurbiprofen, **2a**, **2b**, **3a**, **3b**, **4a**, **4b**, **5b**, and **6b** at 220 and 254 nm.

Ibuprofen



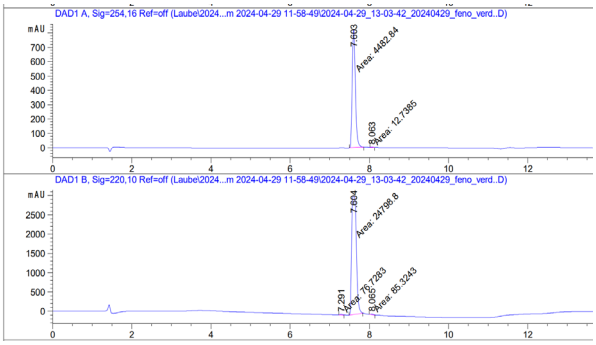
Signal 2: DAD1 A, Sig=254,16 Ref=off

Peak #	RetTime [min]	Type	Width [min]	Area [mAU*s]	Height [mAU]	Area %
1	7.990	MM	0.0890	1124.28564	210.52943	100.00
Totals :				1124.28564	210.52943	

Signal 3: DAD1 B, Sig=220,10 Ref=off

Peak #	RetTime [min]	Type	Width [min]	Area [mAU*s]	Height [mAU]	Area %
1	7.990	MM	0.1330	2.10743e4	2640.41724	100.00
Totals :				2.10743e4	2640.41724	

Fenoprofen



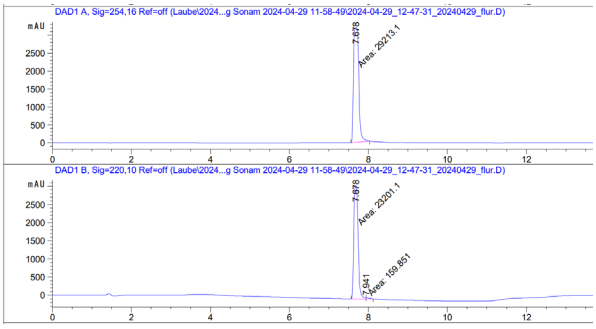
Signal 2: DAD1 A, Sig=254,16 Ref=off

Peak #	RetTime [min]	Type	Width [min]	Area [mAU*s]	Height [mAU]	Area %
1	7.603	MM	0.0905	4482.83789	825.55927	99.7166
2	8.063	MM	0.0762	12.73851	2.78574	0.2834
Totals :				4495.57640	828.34501	

Signal 3: DAD1 B, Sig=220,10 Ref=off

Peak #	RetTime [min]	Type	Width [min]	Area [mAU*s]	Height [mAU]	Area %
1	7.291	MM	0.0811	76.72831	15.77770	0.3074
2	7.604	MM	0.1344	2.47988e4	3074.15088	99.3508
3	8.065	MM	0.0810	85.32430	17.55629	0.3418
Totals :				2.49609e4	3107.48487	

Flurbiprofen



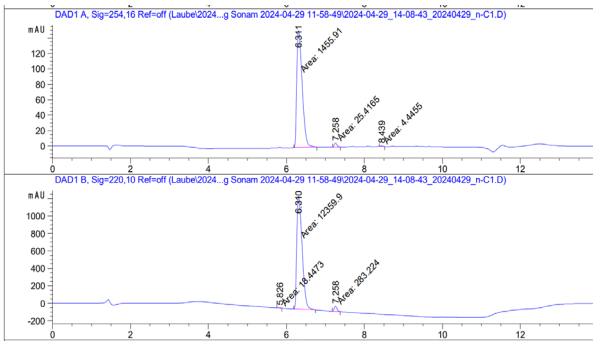
Signal 2: DAD1 A, Sig=254,16 Ref=off

Peak #	RetTime [min]	Type	Width [min]	Area [mAU*s]	Height [mAU]	Area %
1	7.678	MM	0.1520	2.92131e4	3202.78052	100.0000
Totals :				2.92131e4	3202.78052	

Signal 3: DAD1 B, Sig=220,10 Ref=off

Peak #	RetTime [min]	Type	Width [min]	Area [mAU*s]	Height [mAU]	Area %
1	7.678	MF	0.1237	2.32011e4	3126.52539	99.3157
2	7.941	FM	0.0971	159.85115	27.43852	0.6843
Totals :				2.33610e4	3153.96391	

2a



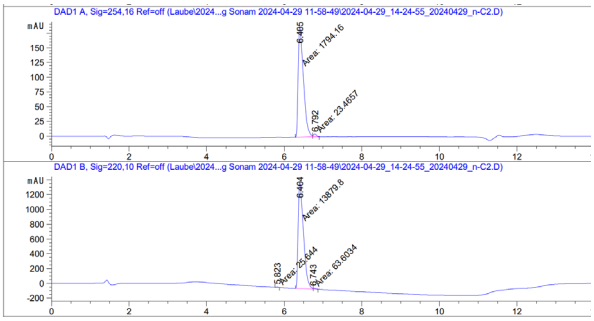
Signal 2: DAD1 A, Sig=254,16 Ref=off

Peak #	RetTime [min]	Type	Width [min]	Area [mAU*s]	Height [mAU]	Area %
1	6.311	MM	0.1597	1455.90918	151.98502	97.9901
2	7.258	MM	0.0808	25.41654	5.24392	1.7107
3	8.439	MM	0.0781	4.44550	9.48431e-1	0.2992
Totals :				1485.77122	158.17736	

Signal 3: DAD1 B, Sig=220,10 Ref=off

Peak #	RetTime [min]	Type	Width [min]	Area [mAU*s]	Height [mAU]	Area %
1	5.826	MM	0.0761	18.44734	4.03816	0.1457
2	6.310	MM	0.1592	1.23599e4	1294.25122	97.6174
3	7.258	MM	0.0792	283.22430	59.61414	2.2369
Totals :				1.26616e4	1357.90352	

2b



Signal 2: DAD1 A, Sig=254,16 Ref=off

Peak #	RetTime [min]	Type	Width [min]	Area [mAU*s]	Height [mAU]	Area %
1	6.405	MF	0.1594	1794.15588	187.58167	98.7090
2	6.792	FM	0.0845	23.46570	4.63022	1.2910

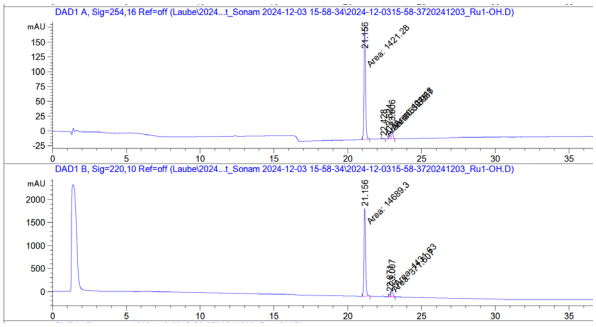
Totals : 1817.62159 192.21188

Signal 3: DAD1 B, Sig=220,10 Ref=off

Peak #	RetTime [min]	Type	Width [min]	Area [mAU*s]	Height [mAU]	Area %
1	5.823	MM	0.0738	25.64400	5.78967	0.1836
2	6.404	MF	0.1602	1.38798e4	1444.28040	99.3611
3	6.743	FM	0.0885	63.60336	11.97167	0.4553

Totals : 1.39690e4 1462.04174

3a



Signal 2: DAD1 A, Sig=254,16 Ref=off

Peak #	RetTime [min]	Type	Width [min]	Area [mAU*s]	Height [mAU]	Area %
1	21.156	MM	0.1248	1421.27747	189.77274	87.3583
2	22.428	MM	0.1407	10.59751	1.25527	0.6514
3	22.824	MF	0.1053	63.89671	10.10933	3.9274
4	23.006	FM	0.1266	131.17989	17.26437	8.0629

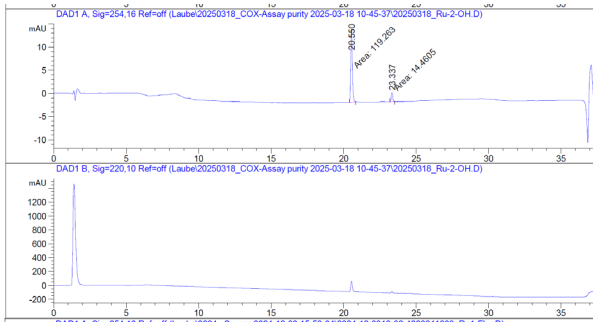
Totals : 1626.95157 218.40170

Signal 3: DAD1 B, Sig=220,10 Ref=off

Peak #	RetTime [min]	Type	Width [min]	Area [mAU*s]	Height [mAU]	Area %
1	21.156	MM	0.1285	1.46893e4	1905.62329	89.0663
2	22.871	MF	0.0993	371.60736	62.36855	2.2532
3	23.007	FM	0.1258	1431.63281	189.72269	8.6805

Totals : 1.64926e4 2157.71452

3b



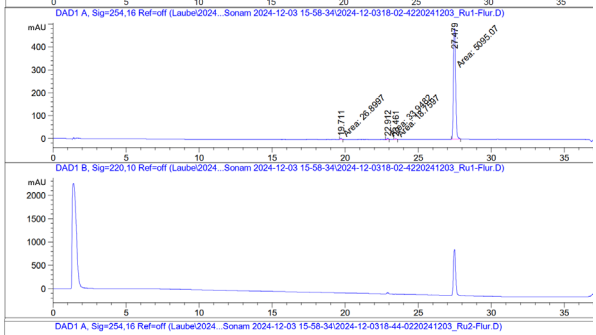
Signal 2: DAD1 A, Sig=254,16 Ref=off

Peak #	RetTime [min]	Type	Width [min]	Area [mAU*s]	Height [mAU]	Area %
1	20.550	MM	0.1259	119.26324	15.78806	89.1863
2	23.337	MM	0.1236	14.46047	1.94960	10.8137

Totals : 133.72372 17.73766

Signal 3: DAD1 B, Sig=220,10 Ref=off

4a



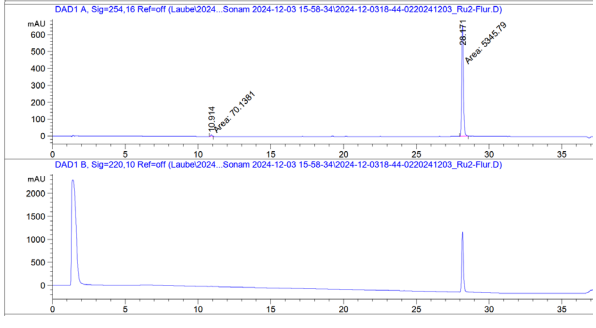
Signal 2: DAD1 A, Sig=254,16 Ref=off

Peak #	RetTime [min]	Type	Width [min]	Area [mAU*s]	Height [mAU]	Area %
1	19.711	MM	0.1192	26.89965	3.76102	0.5198
2	22.912	MM	0.1257	33.94823	4.50294	0.6560
3	23.461	MM	0.1277	18.75972	2.44882	0.3625
4	27.479	MM	0.1752	5095.06641	484.57080	98.4616

Totals : 5174.67401 495.28359

Signal 3: DAD1 B, Sig=220,10 Ref=off

4b



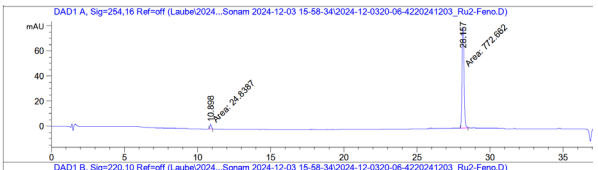
Signal 2: DAD1 A, Sig=254,16 Ref=off

Peak #	RetTime [min]	Type	Width [min]	Area [mAU*s]	Height [mAU]	Area %
1	10.914	MM	0.1183	70.13813	9.87747	1.2950
2	28.171	MM	0.1346	5345.78613	661.90588	98.7050

Totals : 5415.92426 671.78335

Signal 3: DAD1 B, Sig=220,10 Ref=off

5b

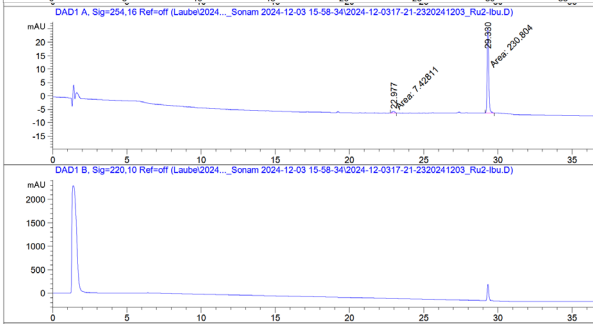


Signal 2: DAD1 A, Sig=254,16 Ref=off

Peak #	RetTime [min]	Type	Width [min]	Area [mAU*s]	Height [mAU]	Area %
1	10.898	MM	0.1141	24.83875	3.62736	3.1146
2	28.157	MM	0.1598	772.66199	80.60784	96.8854
Totals :				797.50073	84.23520	

Signal 3: DAD1 B, Sig=220,10 Ref=off

6b



Signal 2: DAD1 A, Sig=254,16 Ref=off

Peak #	RetTime [min]	Type	Width [min]	Area [mAU*s]	Height [mAU]	Area %
1	22.977	MM	0.2084	7.42811	5.94062e-1	3.1180
2	29.330	MM	0.1206	230.80376	31.90118	96.8820
Totals :				238.23187	32.49524	

Signal 3: DAD1 B, Sig=220,10 Ref=off

11. Evaluation for COX Inhibition

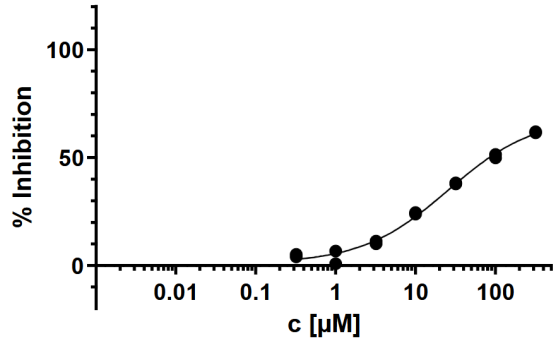


Figure S28. COX-2 inhibition data of **2b**.

12. Dynamic Light Scattering (DLS) Measurements

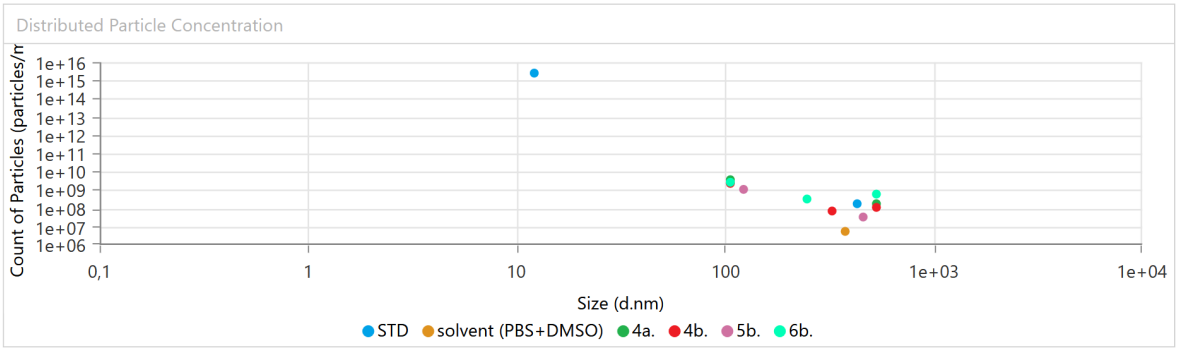


Figure S29: Count of particles of compound **4a**, **4b**, **5b**, and **6b** STD (200 nm) and solvent (DMSO + PBS).

Table S2. Total number concentration and particles concentration peak of compound **4a**, **4b**, **5b**, and **6b** particles (200 nm) and solvent (DMSO + PBS).

Parameter Table

	Sample Name	Particle Concentration Peak One (particles/ml)	Total Number Concentration (particles/ml)
1	STD	2,42E+15	2,42E+15
2	solvent (PBS+DMSO)	5,499E+06	5,499E+06
3	4a.	3,828E+09	4,015E+09
4	4b.	2,172E+09	2,351E+09
5	5b.	1,057E+09	1,093E+09
6	6b.	2,906E+09	3,772E+09

13. Cyclic Voltammetry (CV)

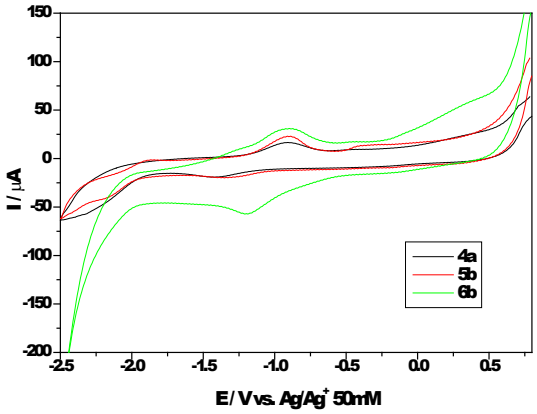
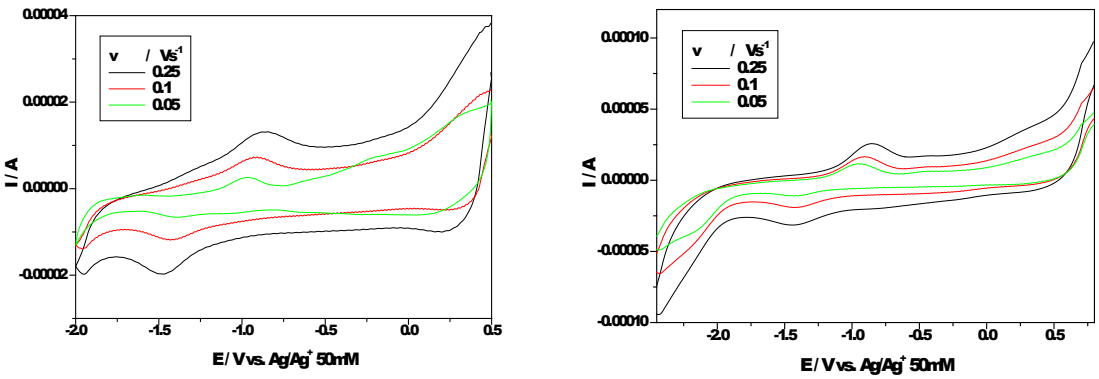
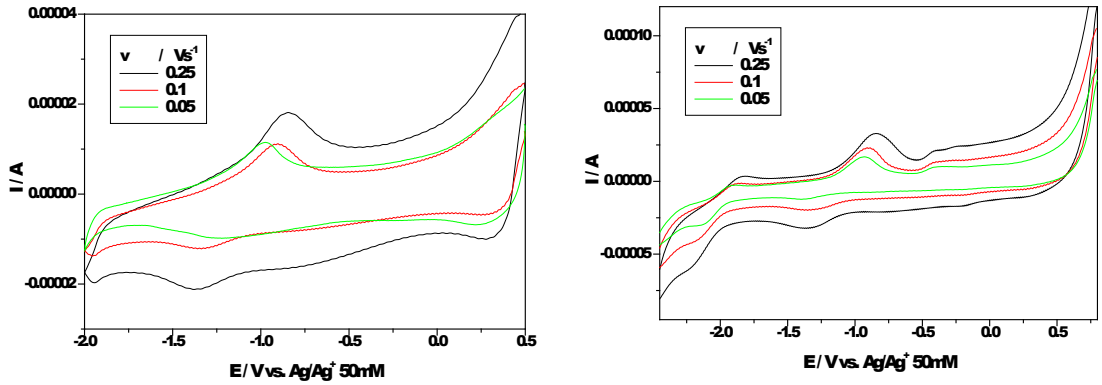


Figure S30. Comparison of CVs obtained for **4a**, **5b**, and **6b**.
Cyclic voltammograms obtained at a Pt electrode with ruthenacarborane-(η^6-*p*-cymene)–NSAID conjugates ($5x10^{-4}$ M). Experimental conditions: 0.1 M [*n*-Bu_4N][PF_6] electrolyte in DMSO solution; scan rate 0.1 V s^{-1}.

4a



5b



6b

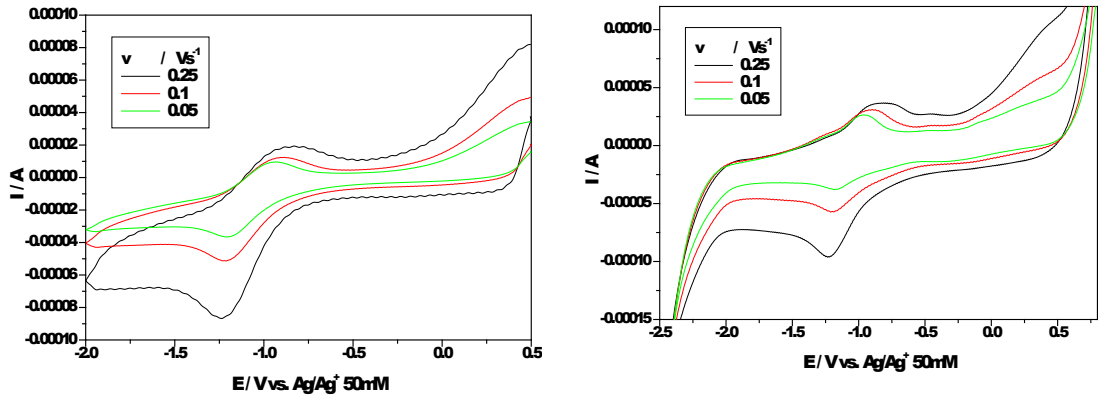


Figure S31. Cyclic voltammograms at different current of 4a, 5b, and 6b.

Peak parameters:

All the potentials presented here are *vs.* $Ag/AgNO_3$ (50 mM) for all the ruthenacarborane-(η^6-*p*-cymene)–NSAID conjugates (in DMSO with 0.1M [*n*-Bu_4N][PF_6]).

The potential against other reference electrodes can be obtained using one of the following relations.

$E[V \text{ vs NHE}] = E[V \text{ vs } Ag/Ag^+] + 0.763$

$E[V \text{ vs } Fc^+/Fc] = E[V \text{ vs } Ag/Ag^+] + 0.123$

14. Cell Viability

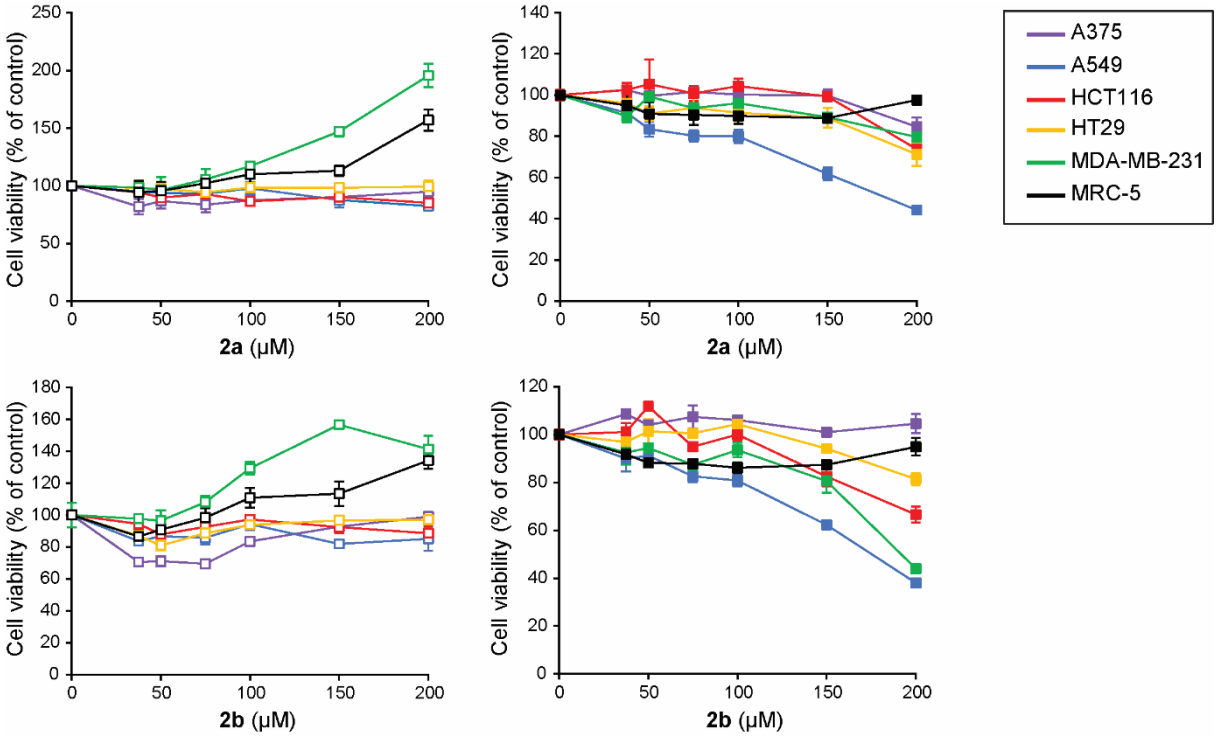


Figure S32. The effect of **2a** and **2b** on the viability of human cancer cell lines and primary transformed lung embryonal fibroblasts. A375 (4×10^3 cells/well), HCT116 (5×10^3 cells/well), HT29 (8×10^3 cells/well), A549 (2×10^3 cells/well), MDA-MB-231 (3×10^3 cells/well), and MRC5 (1×10^4 cells/well) were treated with wide range of concentrations of **2a** and **2b** for 72h, after which the viability was evaluated by MTT (empty squares) and crystal violet test (filled squares). The data are presented as mean ± SD from one representative of three independent experiments and are expressed as a percentage of the viability of untreated cells, which are considered as 100%.

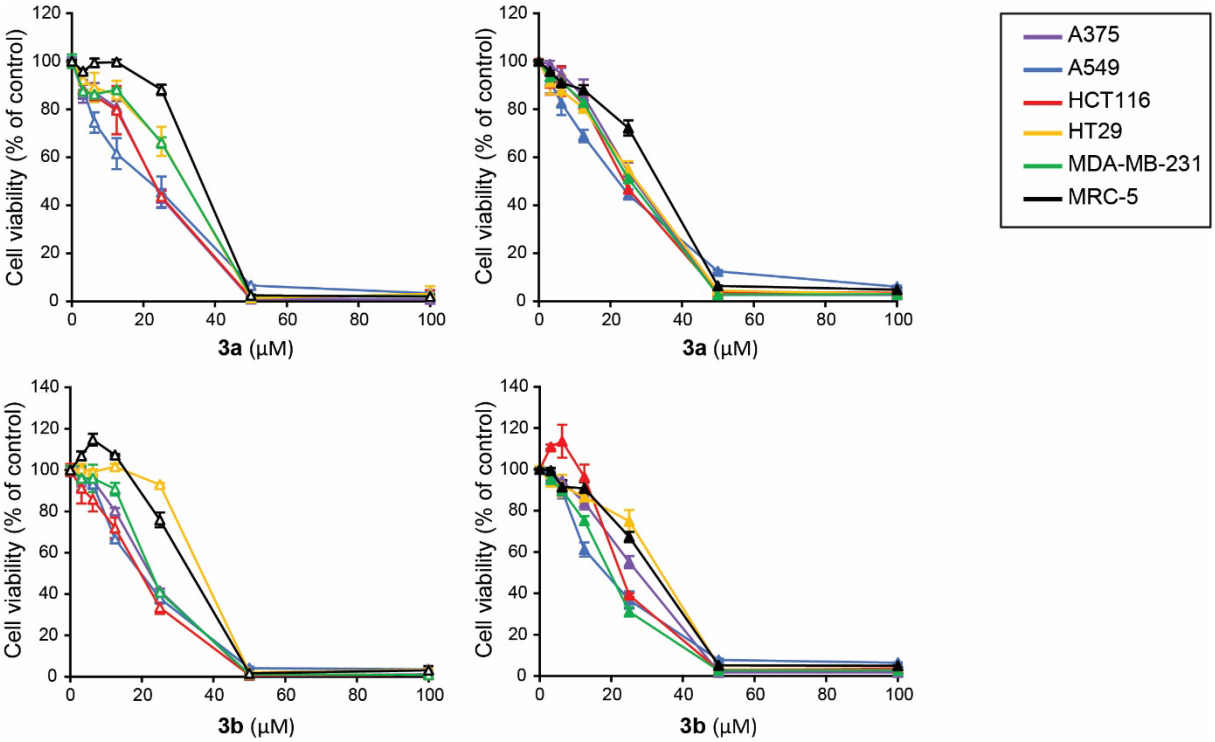


Figure S33. The effect of 3a and 3b on the viability of human cancer cell lines and primary transformed lung embryonal fibroblasts.

A375 (4×10^3 cells/well), HCT116 (5×10^3 cells/well), HT29 (8×10^3 cells/well), A549 (2×10^3 cells/well), MDA-MB-231 (3×10^3 cells/well), and MRC-5 (1×10^4 cells/well) were treated with wide range of concentrations of 3a and 3b for 72h, after which the viability was evaluated by MTT (empty triangles) and crystal violet test (filled triangles). The data are presented as mean ± SD from one representative of three independent experiments and are expressed as a percentage of the viability of untreated cells, which are considered as 100%.

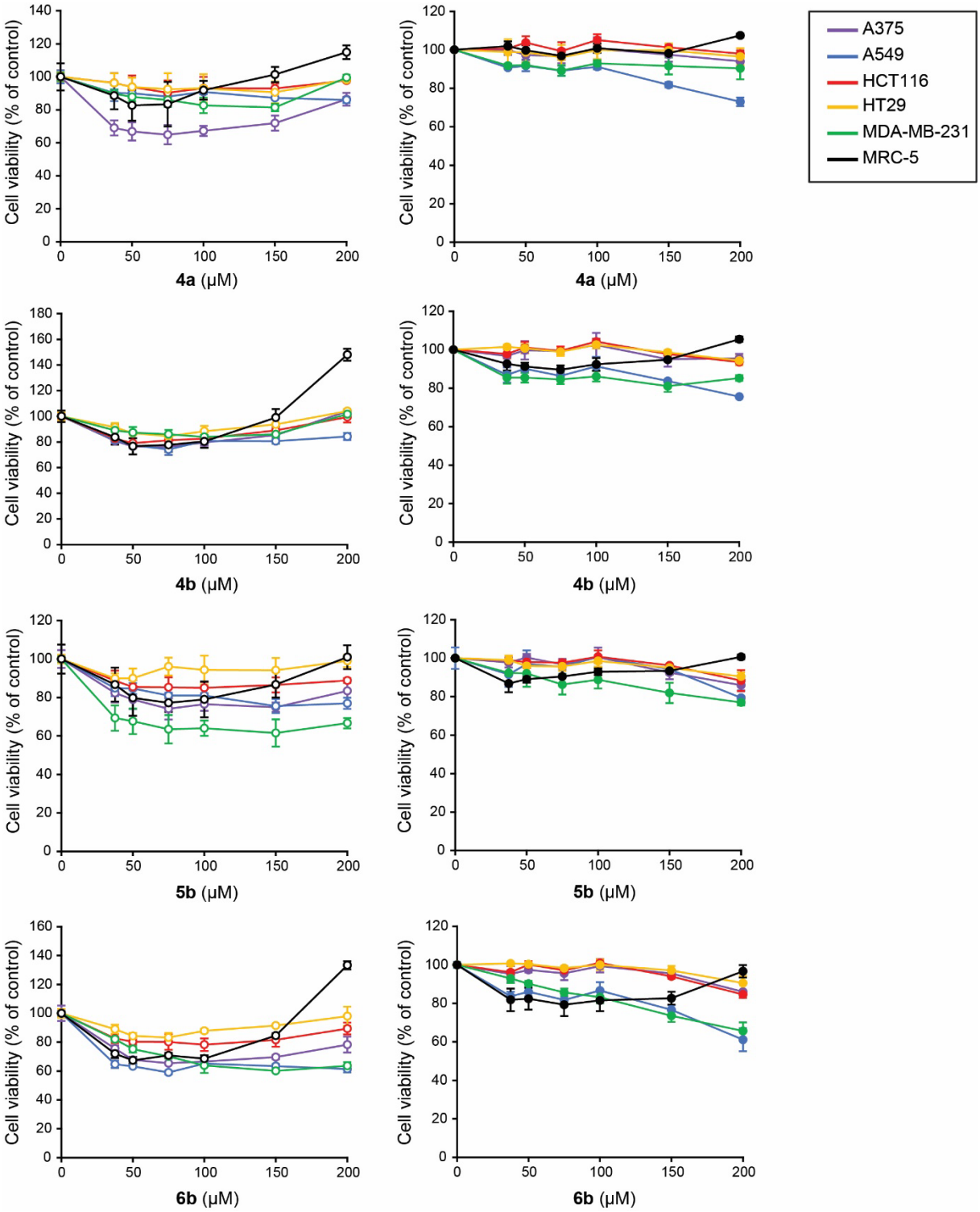


Figure S34. The effect of 4a, 4b, 5b, and 6b on the viability of human cancer cell lines and primary transformed lung embryonal fibroblasts

A375 (4×10^3 cells/well), HCT116 (5×10^3 cells/well), HT29 (8×10^3 cells/well), A549 (2×10^3 cells/well), MDA-MB-231 (3×10^3 cells/well), and MRC-5 (1×10^4 cells/well) were treated with wide range of concentrations of 4a, 4b, 5b, and 6b for 72 h, after which the viability was evaluated by MTT (empty circles) and crystal violet test (filled circles). The data are presented as mean ± SD from one representative of three independent experiments and are expressed as a percentage of the viability of untreated cells, which are considered as 100%.

15. Stability Test by UPLC-MS

Table S3: Stability test by UPLC-MS. Compounds, retention times and m/z.

Compound	t_R in min	m/z used for filter in Da	ion
3a	3.0–3.1	381	$[M + H - H_2O]^+$
3b	3.0–3.1	412	$[M + H]^+$
4a	5.1–5.2	643	$[M + H_2O + H]^+$
5b	5.3–5.4	636	$[M + H]^+$
6b	5.6–5.7	619	$[M + H_2O + H]^+$

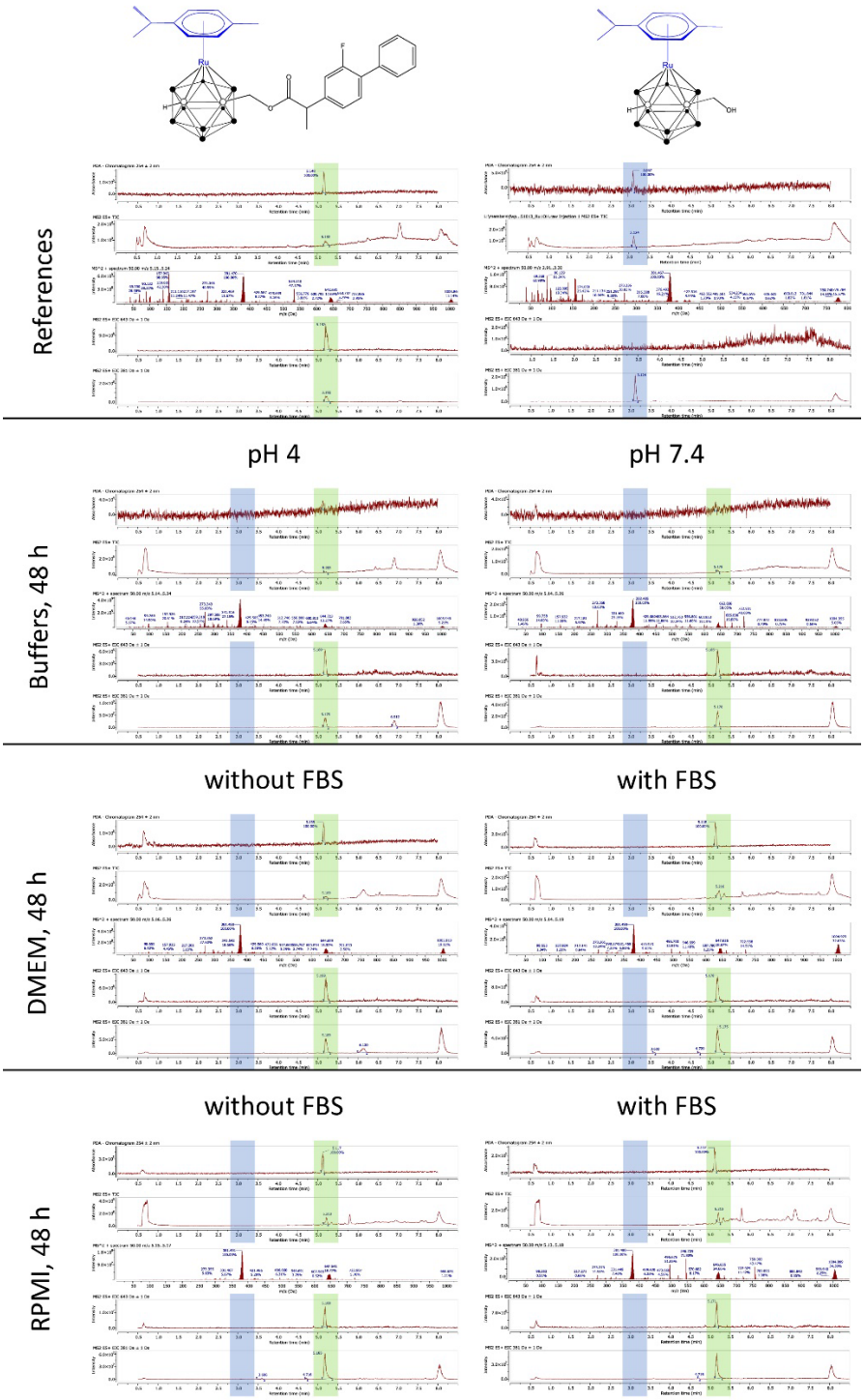


Figure S35: Stability studies of compound **4a** in various media over 48 h.
Each panel is the result of the injection of one sample and is made up of the following chromatograms and spectra (top to bottom): 1) PDA trace at 254 ± 2 nm, 2) total ion count (TIC) chromatogram with integrated peak of **3a** (top right panel) or **4a** (all others), 3) mass spectrum extracted from indicated peak in TIC, 4) TIC filtered for mass peak of **4a** (643 ± 1 Da), 5) TIC filtered for mass peak of **3a** (381 ± 1 Da). The retention times of **4a** (green) and **3a** (blue) are highlighted in all chromatograms. Panels are in the following order: top row) references **4a** (left) and **3a** (right), second row) samples from pH 4 (left) and pH 7.4 (right), third row) samples from DMEM without (left) and with (right) addition of 10 % FBS, bottom row) samples from RPMI without (left) and with (right) addition of 10 % FBS.

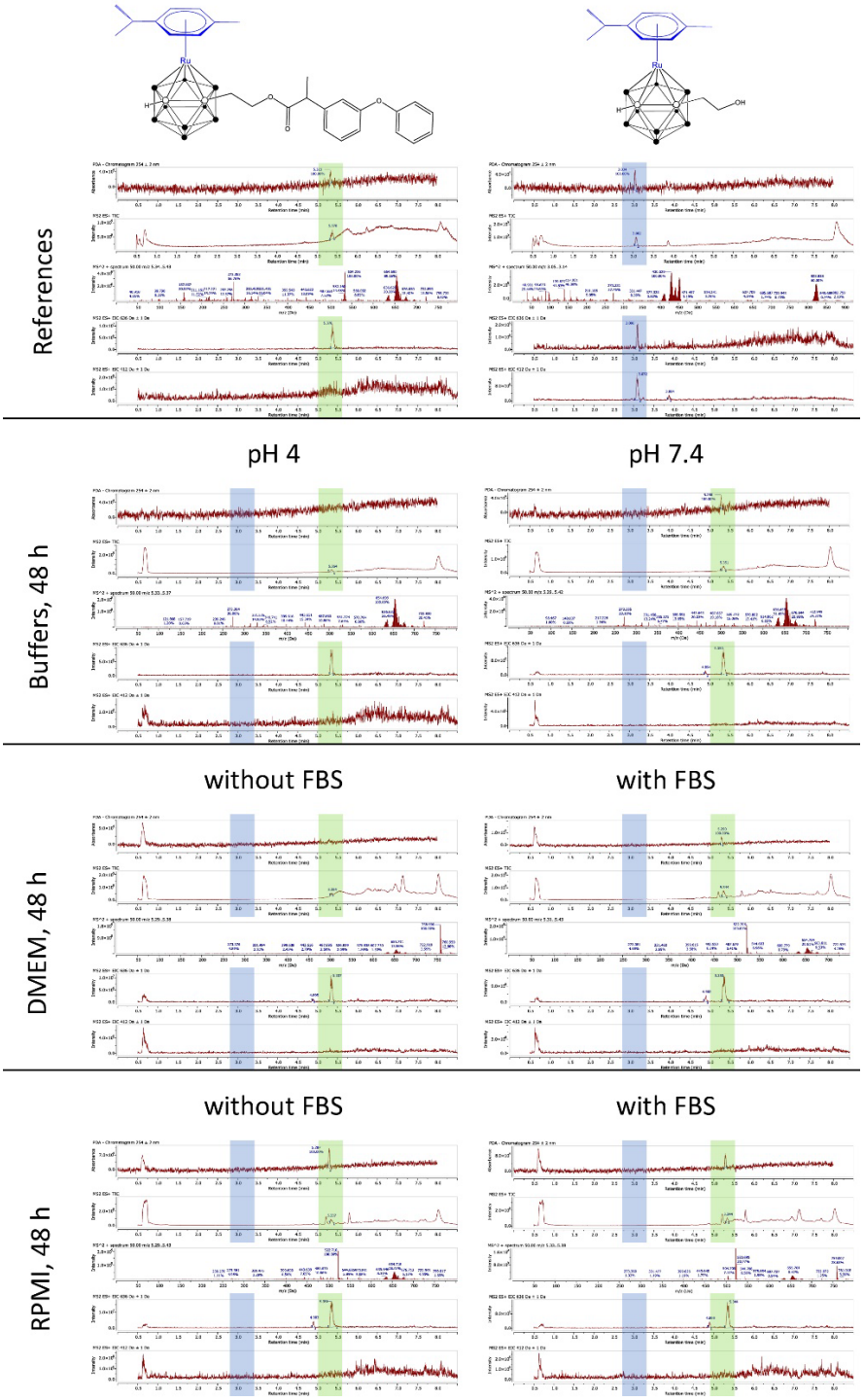


Figure S36: Stability studies of compound **5b** in various media over 48 h.
Each panel is the result of the injection of one sample and is made up of the following chromatograms and spectra (top to bottom): 1) PDA trace at 254 ± 2 nm, 2) TIC chromatogram with integrated peak of **3b** (top right panel) or **5b** (all others), 3) mass spectrum extracted from indicated peak in TIC, 4) TIC filtered for mass peak of **5b** (643 ± 1 Da), 5) TIC filtered for mass peak of **3b** (381 ± 1 Da). The retention times of **5b** (green) and **3b** (blue) are highlighted in all chromatograms. Panels are in the following order: top row) references **5b** (left) and **3b** (right), second row) samples from pH 4 (left) and pH 7.4 (right), third row) samples from DMEM without (left) and with (right) addition of 10 % FBS, bottom row) samples from RPMI without (left) and with (right) addition of 10 % FBS.

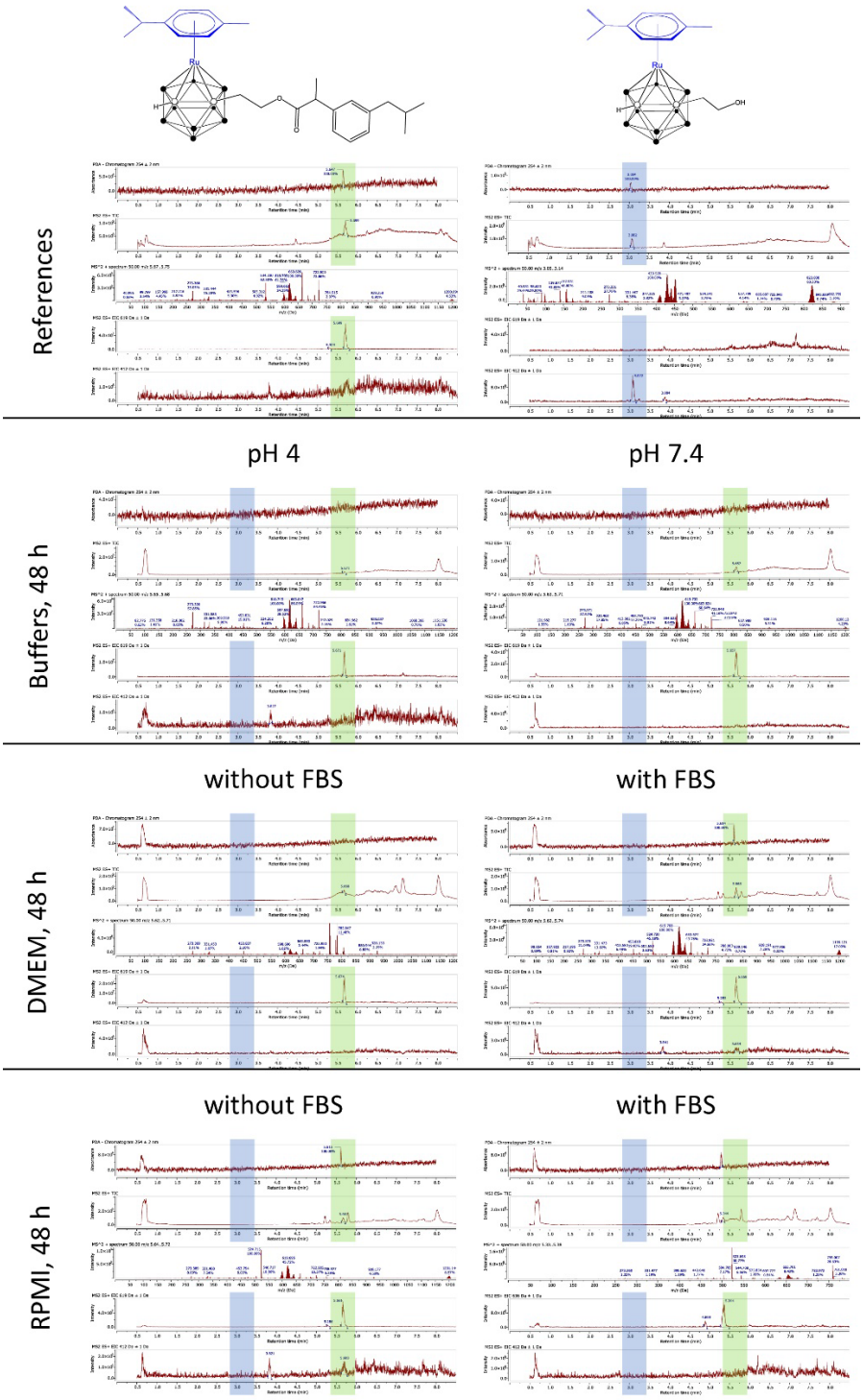


Figure S37: Stability studies of compound **6b** in various media over 48 h.
Each panel is the result of the injection of one sample and is made up of the following chromatograms and spectra (top to bottom): 1) PDA trace at 254 ± 2 nm, 2) TIC chromatogram with integrated peak of **3b** (top right panel) or **6b** (all others), 3) mass spectrum extracted from indicated peak in TIC, 4) TIC filtered for mass peak of **6b** (643 ± 1 Da), 5) TIC filtered for mass peak of **3b** (381 ± 1 Da). The retention times of **6b** (green) and **3b** (blue) are highlighted in all chromatograms. Panels are in the following order: top row) references **6b** (left) and **3b** (right), second row) samples from pH 4 (left) and pH 7.4 (right), third row) samples from DMEM without (left) and with (right) addition of 10 % FBS, bottom row) samples from RPMI without (left) and with (right) addition of 10 % FBS.